# SPECTRAL DISTORTIONS OF THE COSMIC MICROWAVE RADIATION DUE TO INTERACTION WITH THE HOT GAS IN A MOVING CLUSTER: INCLUSION OF RELATIVISTIC EFFECTS

**S.Y. Sazonov and R.A. Sunyaev**

*Space Research Institute, Russian Academy of Sciences, Moscow*

*Max-Planck-Institut fuer Astrophysik, Garching, Germany*

A relativistic treatment of the spectral effects that arise during the passage of the cosmic microwave background (CMB) radiation through intracluster gas due to chaotic motion of electrons (thermal effect) and due to the motion of a galaxy cluster as a whole (kinematic effect) is given. The Monte Carlo simulations which were performed by two different methods (i) confirm the existence of the previously proposed relativistic corrections to the thermal effect of the $(kT_e/m_ec^2)^n$ form , where $T_e$ is the gas temperature, and (ii) provide evidence for the presence of additional corrections related to the cluster peculiar motion; the most important correction is proportional to $V_{\rm r}/c \times kT_e/m_ec^2$, where $V_{\rm r}$ is the radial component of the cluster velocity ($V$). The kinematic effect to an accuracy of $(V/c)^4$ and the "cross" effect ($\propto V_{\rm r}/c \times kT_e/m_ec^2$) are derived analytically. All of the effects under consideration are small and, therefore, additive. The relativistic effects are shown to cause the submillimeter flux from galaxy clusters to increase appreciably. This may faciliate searches for clusters at large redshifts.

## Introduction

Thomson scattering by hot intracluster gas leads to distortions of the cosmic microwave background (CMB) spectrum in the direction of galaxy clusters (Sunyaev and Zel'dovich 1972). Using the diffusion equation of Kompaneets (1957), Zel'dovich and Sunyaev (1969) showed that the magnitude of this "thermal effect" is proportional to the parameter $y = (kT_e/m_ec^2)\tau$, where $T_e$ is the temperature of the thermal motion of the electrons, and $\tau$ is the Thomson optical depth of the cluster along the line of sight. The CMB spectrum must also be distorted by the motion of the cluster as a whole (Sunyaev and Zel'dovich 1980a). The magnitude of this "kinematic effect" is proportional to $\tau V_r/c$, where $V_r$ is the radial component of the cluster peculiar velocity. Changes in the spectral intensity of the CMB caused by the thermal ($\Delta I_\nu^{\rm T}$) and kinematic ($\Delta I_\nu^{\rm K}$) effects are described by the formulas

$$\frac{\Delta I_\nu^{\rm T}}{I_\nu} = y\frac{xe^x}{e^x-1}\left(x\frac{e^x+1}{e^x-1}-4\right), \tag{1}$$

$$\frac{\Delta I_\nu^{\rm K}}{I_\nu} = \tau\frac{V_r}{c}\frac{xe^x}{e^x-1}. \tag{2}$$

The CMB spectral intensity is given by the formula of blackbody radiation

$$I_\nu = \frac{2(kT_R)^3}{(hc)^2}\frac{x^3}{e^x-1}, \tag{3}$$

where $x = h\nu/kT_R$ is a dimensionless frequency. In what follows, $T_R = 2.726$ K is the current CMB temperature (Mather et al., 1994). Recall that the distortion caused by the kinematic effect can be either positive or negative over the entire frequency range, depending on whether the cluster is moving toward us ($V_r > 0$) or away from us ($V_r < 0$).

Formulas (1) and (2) are valid in the nonrelativistic limit. However, the gas temperature ($kT_e$) measured by X-ray telescopes in galaxy clusters ranges from $\sim 3$ to $\sim 17$ keV (Tucker et al. 1998). Therefore, the electron thermal velocities can reach $\sim$ (0.1–0.3) $c$, and, in principle, relativistic effects related to the change in the differential cross-section, the formula that describes the energy transfer between electrons and photons, and the distribution function of electron velocities can show up. The numerical calculations by Rephaeli (1995), which were based on the results of previous studies (Wright 1979; Fabbri 1981; Taylor and Wright 1989; Loeb et al. 1991), showed that the relativistic corrections to formula (1) describing the thermal effect are actually significant in the observed range of gas temperatures and must be taken into account when interpreting measurements of the thermal effect in future experiments, such as Planck Surveyor. Rephaeli (1995) obtained his result by averaging the probability of a change in the photon frequency over a Maxwellian distribution of electron velocities using a single-scattering approximation; this is quite justifiable, because the optical depths of the gas in clusters of galaxies do not

exceed $\tau \sim 0.01$. As was noted by Sunyaev (1980), in general, the diffusion approximation cannot be applied to problems with a small number of scatterings. Indeed, the spectrum of a monochromatic line after the scattering by an optically thin cloud of gas differs markedly from the spectrum that follows from the Kompaneets equation (Sunyaev 1980). Nevertheless, if the incident radiation spectrum is smooth and sufficiently wide (compared to the typical change of the photon frequency in a scattering), the diffusion approximation must hold even in the case of a single scattering (see also Loeb et al. 1991). This fact formed the basis for the studies of Stebbins (1997), Itoh et al. (1998), and Challinor and Lasenby (1998), who derived formulas, written as a series in powers of $kT_e/m_ec^2$, for the thermal effect by expanding the Boltzmann equation in the Fokker-Planck approximation. Their results turned out to be in excellent agreement with the numerical calculations of Rephaeli (1995) over the entire frequency range, with the exception of the far Wien region where the series in powers of $kT_e/m_ec^2$ converges poorly. In this region, the spectral intensity declines exponentially with frequency, and the validity condition for the diffusion approximation is violated (the situation is similar to the scattering of a monochromatic line).

As was noted above, so far two basic approaches have been used when considering the effects that arise during the interaction of the CMB with intracluster gas: the Fokker-Planck approximation of the kinetic equation that describes the redistribution of photons in frequency with time and the numerical method that is detailed in Loeb et al. (1991). At the same time, the stochastic nature of the problem and the small fraction of photons that undergo scatterings provide ideal conditions for using the numerical Monte Carlo method to solve the problem in question. In this paper, we present the results of such calculations, which confirm the results that have been previosly obtained for the thermal effect and which allow us to bound the range of values of $kT_e/m_ec^2$ within which the approximate analytical formulas are applicable. Another prerequisite for initiating this study was a realization of the fact that the relativistic effects must lead to corrections to the kinematic effect similar to those that were found previously for the thermal effect. Our numerical calculations confirmed the existence of an additional spectral distortion, whose magnitude is proportional to $V_r/c \times kT_e/m_ec^2$, and corrections of higher order ($\propto (V/c)^m \times (kT_e/m_ec^2)^n$). Once we obtained the results of the Monte Carlo simulations, we considered the problem analytically and derived formulas that describe the key corrections to the kinematic effect. Their derivation is also given here.

## Monte Carlo Calculations

### *a) The Case of a Cluster at Rest*

Let us first consider the problem in which an isotropic radiation field is scattered by a cloud of electrons at rest. The electron momenta ($\mathbf{p}$) follow a relativistic Maxwellian distribution with temperature $T_e$:

$$dN_e \sim \exp\left[-(p^2c^2 + m_e^2c^4)^{1/2}/kT_e\right] d\mathbf{p}. \tag{4}$$

The incident radiation spectrum is a blackbody one. Using the formulas from the review by Pozdnyakov et al. (1983), which describe the various aspects of Comptonization as applied to the Monte Carlo method, we calculated the spectral distortion that resulted from the passage of the radiation through the cloud of hot electrons for various values of $T_e$. In the problem under consideration, the change of the photon energy in a scattering is almost entirely attributable to the Doppler effect; the contribution from the recoil effect is negligible, because the photon energies are low. In the case of an optically thin scattering medium, and it is this situation that is realized in galaxy clusters, the spectral distortion is largely determined by single scatterings. For this reason, the magnitude of the effect is proportional to the Thomson depth of the cloud along the line of sight: $\tau = \int N_e(r)\sigma_{\rm T}\, dr$.

Fig. 1 shows the dependences that we derived in our simulations for the spectral distortion. They were normalized to the parameter $y$. The spectral dependence that we obtained in the nonrelativistic approximation by using formula (1) is shown in the same figure. We see that, in general, the magnitude of the distortion can no longer be desribed by one parameter $y$ because of the relativistic effects. The expression that describes the spectral change must explicitly contain temperature $T_e$. Our results are in excellent agreement with the results that have been previously obtained by using a different numerical method of Rephaeli (1995). Figure 2 shows how the ratio of the real distortion to that calculated from the nonrelativistic formula (1) increases with increasing $kT_e/m_ec^2$ for various frequencies $x$. The great flux increase in the far Wien spectral region ($kT_e/m_ec^2 = 17$ keV, by 30% at $x = 10$ and by 90% at $x = 12$) is worthy of special note. In Table 1, which was compiled from the results of our Monte Carlo calculations, the magnitude of the additional CMB distortion (minus the distortion described by formula (1)) is given as a function of $x$ and $kT_e/m_ec^2$.

Figures 3–5 compare the spectra obtained by the Monte Carlo method with those calculated by using an analytical formula (Itoh et al. 1998) for three values of the gas temperature: $kT_e/m_ec^2 = 0.02$, 0.03, and 0.04. Figures 6 and 7 show the regions in the ($x$, $kT_e/m_ec^2$) plane within which the deviation of the approximate solution (Itoh et al. 1998) from the exact one is no greater than 5% and 10%, respectively. On each of these graphs, the comparison is made with polynomials that include a variable number of the first terms of the expansion in $kT_e/m_ec^2$. We conclude that the analytical expression (when the first 2 to 4 terms are included) is an excellent approximation in the range of moderate frequencies up to the highest temperatures ($kT_e/m_ec^2 \sim 17$ keV) that have ever been measured in galaxy clusters. Nevertheless, the deviations become significant in the far Wien spectral region ($x \gtrsim 10$). For this reason, the numerically obtained values (see Table 1) must be used to interpret measurements of the thermal effect at submillimeter wavelengths. Itoh et al. (1998) also point out the poor convergence of their series at high x.

*b) A Cluster is Nonuniform in $T_e$*

In the case of a real galaxy cluster, the cloud of gas is inhomogeneous: the density and temperature of the gas change both along the line of sight and in the direction within the solid angle in which the measurements are carried out. The total distortion is a

superposition of the distortions produced by inidividual monotemperature gas regions. In the Wien part of the spectrum, the contribution of hot regions dominate, because the relativistic corrections are especially important at high frequencies. In the general case, the distortion can be written as a series in powers of $kT_e/m_ec^2$:

$$\delta I_\nu = f(x)\int \frac{kT_e(\tau)}{m_ec^2}\,d\tau + g(x)\int\left(\frac{kT_e^2(\tau)}{m_ec^2}\right)^2 d\tau + h(x)\int\left(\frac{kT_e^3(\tau)}{m_ec^2}\right)^3 d\tau + ..., \qquad (5)$$

where the function $f(x)$ describes the linear effect (see formula (1)), $g(x)$ describes the quadratic effect, etc., and the integrals are taken along the line of sight. We can try to fit a model monotemperature cloud with $T_e^m$ and $\tau^m$ to this expression. The distortion caused by such a cloud is

$$\delta I_\nu^m = f(x)\tau^m\frac{kT_e^m}{m_ec^2} + g(x)\tau^m\left(\frac{kT_e^m}{m_ec^2}\right)^2 + h(x)\tau^m\left(\frac{kT_e^m}{m_ec^2}\right)^3 + \dots . \qquad (6)$$

We can find the values of $T_e^m$ and $\tau^m$ at which the difference between the model and actual spectra is $O((kT_e^m(\tau)/m_ec^2)^3)$. To this end, we must equate the coefficients of $f(x)$ and $g(x)$ in relations (5) and (6) and then solve the resulting system of two linear equations. As a result, we obtain

$$T_e^m = \frac{\int T_e^2(\tau)\,d\tau}{\int T_e(\tau)\,d\tau}; \quad \tau^m = \frac{(\int T_e(\tau)\,d\tau)^2}{\int T_e^2(\tau)\,d\tau}. \qquad (7)$$

.

As an example, Fig. 8 shows the distortion spectrum that results after the passage of the CMB through two gas layers: the first with $(kT_e/m_ec^2)_1 = 0.01$ and the second with $(kT_e/m_ec^2)_1 = 0.03$, both having the same optical depth $\tau_1 = \tau_2 = 0.5\tau_0$. In the same figure, the data are fitted by a one-component model with the parameters $kT_e^m/m_ec^2 = 0.025$ and $\tau^m = 0.8\tau_0$ which were obtained from formulas (7). We see that the model is in remarkable agreement with the data; the discrepancies become appreciable only in the far Wien spectral region ($x \gtrsim 25$). Thus, although the thermal effect is a separable function of $kT_e/m_ec^2$ and $\tau$ due to the relativistic corrections, it is difficult to obtain unequivocal information on the distribution of $T_e$ over a galaxy cluster by using microwave measurements alone. As before (as in the case of the linear effect), data from X-ray observations must be invoked. It also follows from the above discussion that the distortion spectrum can be readily calculated for a cloud of gas with any given $T_e(\tau)$ distribution, provided the tabulated dependences are available for several values of $kT_e/m_ec^2$.

### *c) Allowance for the Finite Optical Depth of a Cluster*

In our calculations, we also tested clouds of electrons with various optical depths by taking into account multiple scatterings. It is easy to show that the contribution to the total

spectral distortion from the secondary scatterings of photons must be proportional to $y^2$. The spectral shape of this additional distortion can be determined by substituting the spectrum that results after the first scattering, which is given by formula (1), into the Kompaneets equation. By differentiation with respect to frequency, we obtain

$$\frac{\delta I_\nu}{I_\nu} \sim y^2 \frac{xe^x}{e^x-1}\left[-16+34x\coth(x/2)-12x^2\left(\coth^2(x/2)+\frac{1}{2\sinh^2(x/2)}\right)\right.$$
$$\left.+x^3\coth(x/2)\left(\coth^2(x/2)+\frac{2}{\sinh^2(x/2)}\right)\right] \qquad (8)$$

This relation must be preceded by the coefficient $\sim 1$ which depends on the distribution of electrons over the cloud and on the direction in which the measurements are made. For typical values of $\tau$ ($\sim 0.01$), we see that the additional distortion is negligible. Even in the case of a very large depth $\tau \sim 0.1$, the correction proportional to $y^2$ turns out to be one order of magnitude smaller than the principal relativistic correction proportional to $y(kT_e/m_ec^2)$ over the entire frequency range. The effect of multiple scatterings in the problem under consideration can therefore be ignored. Our numerical calculations fully confirm this conclusion.

*d) Allowance for the Peculiar Motion of a Cluster*

A change from the simple situation in which the cluster is at rest to the problem in which the cluster moves relative to the CMB can be made in terms of the Monte Carlo method in two different ways. In the first approach, we work in the laboratory frame (which is at rest with respect to the CMB), in which the initial radiation field remains the same as in the case of a cluster at rest (isotropic, with a Planck spectrum). As before, the electron velocities are drawn from a Maxwellian distribution, but this time in the frame of reference in which the cluster is at rest. Using the property of invariance of the distribution function in phase space (see, e.g., Landau and Lifshitz 1988), we can convert the electron momenta from the cluster rest frame ($\mathbf{p}_0$) to the laboratory frame ($\mathbf{p}$) by means of the Lorentz transformations

$$p_x = \gamma\left[p_{x0}+\frac{V}{c^2}(p^2c^2+m_e^2c^4)^{1/2}\right]; \quad p_y = p_{y0}; \quad p_z = p_{z0}, \qquad (9)$$

where $\gamma = (1-V^2/c^2)^{-1/2}$, and the $X$ axis is directed along the cluster velocity $\mathbf{V}$. Next, the scattering of a photon by an electron is drawn in the standard fashion.

In the second approach, the scatterings of photons are drawn in the cluster rest frame. In this frame, the spectrum of the incident radiation remains a blackbody one, but its temperature depends on the angle of incidence: $T_{R0} = T_R/\gamma/(1+V\cos\theta_0/c)$. Once the spectral distortion has been calculated in the cluster rest frame, we can determine the corresponding quantity in the laboratory frame by using formulas (11), (19), and (20), which are given below. We performed the calculations by both methods and obtained

identical results, as one might expect. We used the following model parameters $kT_e/m_ec^2$, $V/c$, $\mu = \cos\theta$, where $\theta$ is the angle between the velocity vector and the vector directed from the cluster to the observer. The optical depth of the cluster was assumed to be small (only single scatterings were taken into account).

The Monte Carlo simulations revealed additional, previously unknown relativistic corrections to the thermal and kinematic effects due to the peculiar motions. In addition to the correction terms which are proportional to different powers of $V/c$ and which are the same as in the case of a cold cloud of gas ($T_e = 0$), there are "cross" terms, the main of which is proportional to $V_r/c \times kT_e/m_ec^2$. Having found additional corrections by our Monte Carlo calculations, we undertook an analytical treatment of the problem and derived simple formulas that describe the spectrum of the additional distortions; their derivation is given below.

Figures 9 and 10 show the spectra of the total CMB distortion in the direction of the cluster of galaxies for $kT_e/m_ec^2 = 0.02$ and $V/c = 0.01$ in two cases: the cluster moves toward us ($\mu = 1$) and away from us ($\mu = -1$). For demonstration purposes, the cluster velocity (3000 km/s) was chosen to be somewhat higher than the actually observed values. The contributions from the terms that are linear and quadratic in $V/c$ and $kT_e/m_ec^2$ and from the cross term $\propto V_r/c \times kT_e/m_ec^2$ are also shown on the graphs. The purely thermal corrections were calculated by using the formulas from Itoh et al. (1998), whereas the corrections whose origin is related to the peculiar motion were derived here (see the following section).

For future measurements of the kinematic and thermal effects, of greatest interest among the newly obtained results is the relativistic correction of the order of $V_r/c \times kT_e/m_ec^2$. Figure 11 shows the spectra of the distortion due to the cross terms alone for a fixed value of the velocity, $V_r/c = 0.01$, and various values of $kT_e/m_ec^2$. We obtained these dependences by subtracting the contribution of the thermal effect and all its relativistic corrections (using our Monte Carlo calculations for a cluster with $V_r = 0$) and the contribution of the kinematic effect (determined for $T_e = 0$) from the spectrum of the total distortion (see Fig. 9 and 10). The dependences for different temperatures were normalized to $V_r/c \times kT_e/m_ec^2$. The same figure shows the frequency dependence of the coefficient of the term $V_r/c \times kT_e/m_ec^2$ in formula (25). We see that this analytical expression provides a good fit to the "accurate" numerical data at moderate gas temperatures ($kT_e/m_ec^2 \lesssim 0.02$). At higher temperatures, the contribution to the distortion that is related to the correction terms of the form $V_r/c \times (kT_e/m_ec^2)^n$ with $n$ = 2,3..., becomes important, especially in the far Wien spectral region.

Fig. 12 also shows the spectra of the distortion due to the cross terms, but for a fixed value of the temperature ($kT_e/m_ec^2 = 0.02$) and various values of $V_r/c$. We see that the effect of the corrections of the form $(V_r/c)^n \times kT_e/m_ec^2$, $n$ = 2,3..., is minor even at very large values of $V_r/c$ ($\sim 0.05$), and that the deviation of the Monte Carlo spectra from the analytical relation is mainly attributable to the term of order $V_r/c \times (kT_e/m_ec^2)^2$ (see Fig. 11).

The results of our Monte Carlo calculations of the cross effect (the sum of corrections of the form $V_r/c \times (kT_e/m_ec^2)^n$) as a function of $x$ and $kT_e/m_ec^2$ are summarized in Table 2.

The main conclusion that can be drawn from the above treatment is that, when analyzing the CMB spectral distortions measured in the direction of moving clusters with hot gas, we must take into account a correction of the order of $V_r/c \times kT_e/m_ec^2$, in addition to the thermal effect and its main relativistic corrections and the kinematic effect. An interesting feature of the additional distortion related to this correction is that its magnitude reaches a local maximum at $x = 3.34$, i.e., near the frequency ($x_c \sim 3.83$) where the thermal effect is at a mimimum and where it is convenient to make measurements of the cluster peculiar velocities on the basis of the kinematic effect. In the frequency range $x \sim 3$–$4$, the correction proportional to $V_r/c \times kT_e/m_ec^2$ causes the magnitude of the kinematic effect to systematically decrease by $\sim 4 \cdot 10^2 (kT_e/m_ec^2)\%$.

Note also that both the kinematic and cross effects can be attributed not only to the motion of the galaxy cluster as a whole, but also to the asymmetrical bulk motions within the cluster, which arise, for example, in the central regions of clusters (cooling flows) or in a merger of clusters. In this case, the two effects turn out to be proportional to the integral $\int V_r/c\, d\tau$ (at $T_e = const$) taken along the line of sight.

## Analytical Derivation of the Main Relativistic Corrections

### *a) CMB Scattering by a Directed Beam of Electrons (a Moving Cluster with Cold Gas)*

Let us consider the problem of CMB scattering by a directed beam of monoenergetic electrons with density $N_e$ moving at velocity $\mathbf{v}$. We use two frames. The quantities with subscript "0" refer to the frame where the electrons are at rest, whereas the quantities with no subscript are measured in the laboratory frame that is linked to the CMB. In the laboratory frame, the initial occupation number in the phase space of photons is given by Planck's function

$$n = 1/(e^x - 1). \tag{10}$$

The occupation number is invariant with respect to the Lorentz transformations of the frequency and the direction of motion of a photon:

$$\nu_0 = \frac{\nu}{\gamma(1 + \beta\mu_0)} = \nu\gamma(1 - \beta\mu); \quad \mu_0 = \frac{\mu - \beta}{1 - \beta\mu}, \tag{11}$$

where $\beta = v/c$, $\gamma = (1 - \beta^2)^{-1/2}$, $\mu = \cos\theta$, and $\theta$ is the angle between the vector $\mathbf{v}$ and the photon velocity vector (Landau and Lifshitz 1988). Consequently, in the electron rest frame, the occupation number depends on the direction from which the photon came:

$$n_0 = \frac{1}{e^{x_0\gamma(1+\beta\mu_0)} - 1}. \tag{12}$$

Ignoring the recoil effect and the contribution of induced scatterings, we can write the kinetic equation that describes the redistribution of photons in frequency with time in the cluster rest frame:

$$\frac{d}{dt_0} n_0(\mu_0, \nu_0) = cN_{\rm e0} \int \frac{d\sigma}{d\Omega_0'} [n_0(\mu_0', \nu_0) - n_0(\mu_0, \nu_0)]\, d\Omega_0'. \tag{13}$$

In this formula, the Thomson differential cross section is used (the electrons are at rest), which is given by

$$\frac{d\sigma}{d\Omega_0'} = \frac{3\sigma_{\rm T}}{16\pi}(1 + \cos^2\alpha_0), \tag{14}$$

where the scattering angle $\alpha_0$ satisfies the equation

$$\cos\alpha_0 = \mu_0\mu_0' + \sqrt{1-\mu_0^2}\sqrt{1-\mu_0'^2}\cos(\phi_0 - \phi_0'). \tag{15}$$

Intergrating the scattering cross section over the azimuthal angle $(\phi_0 - \phi_0')$, we obtain

$$\frac{d}{dt_0} n_0(\mu_0, \nu_0) = \frac{3cN_{\rm e0}\sigma_{\rm T}}{16} \int_{-1}^{1} (3 + 3\mu_0^2\mu_0'^2 - \mu_0^2 - \mu_0'^2)[n_0(\mu_0', \nu_0) - n_0(\mu_0, \nu_0)]\, d\mu_0'. \tag{16}$$

Next, we expand the expression in the square brackets in a series in powers of $\beta$ up to the fourth order:

$$\begin{aligned}
\frac{n_0(\mu_0', \nu_0) - n_0(\mu_0, \nu_0)}{n_0(\mu_0, \nu_0)} = \frac{e^{x_0\gamma}}{e^{x_0\gamma} - 1} \Bigg[ & x_0\gamma\beta(\mu_0 - \mu_0') + \frac{x_0^2\gamma^2\beta^2}{2}(\mu_0^2 - \mu_0'^2) + \frac{x_0^3\gamma^3\beta^3}{6}(\mu_0^3 - \mu_0'^3) \\
& + \frac{x_0^4\gamma^4\beta^4}{24}(\mu_0^4 - \mu_0'^4)\Bigg] + \left(\frac{e^{x_0\gamma}}{e^{x_0\gamma} - 1}\right)^2 \Bigg[ x_0^2\gamma^2\beta^2(\mu_0'^2 - \mu_0\mu_0') + \frac{x_0^3\gamma^3\beta^3}{2}(2\mu_0'^3 - \mu_0\mu_0'^2 - \mu_0^2\mu_0') \\
& + \frac{x_0^4\gamma^4\beta^4}{12}(7\mu_0'^4 - 2\mu_0\mu_0'^3 - 3\mu_0^2\mu_0'^2 - 2\mu_0^3\mu_0')\Bigg] + \left(\frac{e^{x_0\gamma}}{e^{x_0\gamma} - 1}\right)^3 \Big[ x_0^3\gamma^3\beta^3(-\mu_0'^3 + \mu_0\mu_0'^2) \\
& + \frac{x_0^4\gamma^4\beta^4}{2}(-3\mu_0'^4 + 2\mu_0\mu_0'^3 + \mu_0^2\mu_0'^2)\Bigg] + \left(\frac{e^{x_0\gamma}}{e^{x_0\gamma} - 1}\right)^4 x_0^4\gamma^4\beta^4(\mu_0'^4 - \mu_0\mu_0'^3)
\end{aligned} \tag{17}$$

After the integration over $d\mu_0'$ and the expansion of $\gamma$ in powers of $\beta$, we obtain

$$\frac{1}{n_0(\mu_0,\nu_0)}\frac{dn_0(\mu_0,\nu_0)}{dt_0} = cN_{\rm e0}\sigma_{\rm T}\left\{\frac{x_0e^{x_0}}{e^{x_0}-1}\left[\mu_0\beta+\frac{3(-1+3\mu_0^2)}{20}x_0\beta^2+\frac{\mu_0}{2}\beta^3+\frac{\mu_0}{2}x_0\beta^3\right.\right.$$
$$\left.+\frac{\mu_0^3}{6}x_0^2\beta^3+\frac{3(-1+3\mu_0^2)}{20}x_0\beta^4+\frac{3(-1+3\mu_0^2)}{40}x_0^2\beta^4+\frac{-6-3\mu_0^2+35\mu_0^4}{840}x_0^3\beta^4\right]$$
$$+\left(\frac{x_0e^{x_0}}{e^{x_0}-1}\right)^2\left[\frac{3+\mu_0^2}{10}\beta^2-\frac{\mu_0}{2}\beta^3-\frac{\mu_0(3+\mu_0^2)}{20}x_0\beta^3+\frac{3+\mu_0^2}{10}\beta^4+\frac{3-\mu_0^2}{8}x_0\beta^4\right.$$
$$\left.+\frac{4-\mu_0^2-\mu_0^4}{40}x_0^2\beta^4\right]+\left(\frac{x_0e^{x_0}}{e^{x_0}-1}\right)^3\left[\frac{\mu_0(3+\mu_0^2)}{10}\beta^3-\frac{3+\mu_0^2}{10}\beta^4\right.$$
$$\left.\left.+\frac{-36+3\mu_0^2+7\mu_0^4}{140}x_0\beta^4\right]+\left(\frac{x_0e^{x_0}}{e^{x_0}-1}\right)^4\left[\frac{3(2+\mu_0^2)}{35}\beta^4\right]\right\}. \quad (18)$$

The property of invariance of the occupation number with respect to the Lorentz transformations enables us to determine the corresponding scattering rate in the laboratory frame:

$$\frac{dn(\mu,\nu)}{dt} = \frac{1}{\gamma(1+\beta\mu_0)}\frac{dn_0(\mu_0,\nu_0)}{dt_0}. \quad (19)$$

We must also relate the electron number densities in the two frames, which can be easily done by using the Lorentz transformation of the volume:

$$N_{e0} = N_e/\gamma. \quad (20)$$

Substituting relations (11), (19), and (20) into equation (18), we obtain

$$\frac{1}{n(\mu,\nu)}\frac{dn(\mu,\nu)}{dt} = cN_{\rm e}\sigma_{\rm T}\frac{xe^x}{e^x-1}\left\{\beta\mu+\beta^2\left[-1-\mu^2+\frac{3+11\mu^2}{20}x\coth(x/2)\right]\right.$$
$$+\beta^3\mu\left[2-\frac{31+11\mu^2}{20}x\coth(x/2)+\frac{9+13\mu^2}{120}x^2\left(2\coth^2(x/2)+\frac{1}{\sinh^2(x/2)}\right)\right]$$
$$+\beta^4\left[-1-\mu^2+\frac{17+53\mu^2}{20}x\coth(x/2)-\frac{9+66\mu^2+13\mu^4}{120}x^2\left(2\coth^2(x/2)+\frac{1}{\sinh^2(x/2)}\right)\right.$$
$$\left.\left.+\frac{3+33\mu^2+28\mu^4}{420}x^3\coth(x/2)\left(\coth^2(x/2)+\frac{2}{\sinh^2(x/2)}\right)\right]\right\}. \quad (21)$$

The derived relation describes the kinematic effect for any moving gas cloud (not necessarily a monoenergetic one) which is accurate to the fourth order in $\beta = V/c$, where $V$ is the peculiar velocity. For comparison, formula (2) describes only the linear kinematic

effect (of the order $V_r/c$). Figure 13 shows how the kinematic effect varies with $V/c$ (at $\mu = 1$). If the peculiar velocity of a galaxy cluster does not exceed $V/c \sim 0.01$, then, as follows from Fig. 13, the linear approximation provides an accuracy better than 10% up to $x \sim 15$. For this reason, experimental detection of the distortions caused by the corrections to the kinematic effect (not related to the thermal motion of electrons) seems unlikely. Nevertheless, their inclusion may prove to be necessary in other astrophysical situations, specifically, in those where rapid macro motions of the scattering medium arise, for example, near accreting compact objects.

Compton scattering conserves the total number of photons. We performed a test which confirmed that the terms of all powers of $\beta$ in equation (21) vanish after the integration: $d/dt \int n\nu^2 \, d\nu \, d\mu = 0$. Another well-known integrated characteristic of Compton scattering is the rate of energy transfer between an electron and an isotropic radiation field. The radiation energy density $\epsilon_{\rm r}$ (see, e.g., Pozdnyakov et al. 1983) must increase with time as

$$\frac{d\epsilon_{\rm r}}{dt} = \frac{4}{3} c N_e \sigma_{\rm T} \epsilon_{\rm r} (\gamma^2 - 1). \tag{22}$$

By performing an integral $d/dt \int n \, \nu^3 \, d\nu \, d\mu$ we find in our case:

$$\frac{d\epsilon_{\rm r}}{dt} = \frac{4}{3} c N_e \sigma_{\rm T} \epsilon_{\rm r} (\beta^2 + \beta^4), \tag{23}$$

which is equivalent to relation (22) to an accuracy of the fourth order in $\beta$.

*b) CMB Scattering by a Moving Cloud of Hot Electrons*

Let us now consider a cloud of electrons that moves with a peculiar velocity $V$ at an angle $\theta$ ($\mu = \cos\theta$) to the direction toward the observer. In the cloud rest frame, the electron momenta obey a relativistic Maxwellian distribution with temperature $T_e$, which is given by formula (4), where $\mathbf{p}_0$ should be used instead of $\mathbf{p}$. The corresponding distribution in the laboratory frame is determined by using the Lorentz transformations for the momentum (see formula (9)). We can expand the resulting distribution in a series in powers of $V/c$ and $kT_e/m_e c^2$ to obtain (we restricted ourselves to the corrections that are linear in $kT_e/m_e c^2$ and $V/c$)

$$dN_e = \left(\frac{m_e}{2\pi k T_e}\right)^{3/2} N_e \left(1 + \frac{15 k T_e}{8 m_e c^2}\right)^{-1} \left\{1 + \frac{5V(v_x - V)}{c^2} + \frac{5[(v_x - V)^2 + v_y^2 + v_z^2]}{2c^2} - \frac{3 m_e [(v_x - V)^2 + v_y^2 + v_z^2]^2}{8 c^2 k T_e} - \frac{m_e V (v_x - V)[(v_x - V)^2 + v_y^2 + v_z^2]}{c^2 k T_e}\right\} \times \exp\left\{-\frac{m_e[(v_x - V)^2 + v_y^2 + v_z^2]}{2 k T_e}\right\} dv_x \, dv_y \, dv_z, \tag{24}$$

where $v_x$, $v_y$, $v_z$ are the components of electron velocity, with the $X$ axis being directed along $\mathbf{V}$.

Let us choose the $Y$ axis in the plane that is formed by the vectors $\mathbf{V}$ and $\mathbf{l}$, where $\mathbf{l}$ is a unit vector directed from the cluster to the observer. In this case, $(\mathbf{v}/c, \mathbf{l}) = (v_x/c)\mu + (v_y/c)\sqrt{1-\mu^2}$. Substituting this expression for $\beta\mu$ and $(v_x^2 + v_y^2 + v_z^2)/c^2$ for $\beta^2$ into equation (21) we obtain after averaging over (24) (the integrals of the form $\int v_y ... \, dv_x \, dv_y \, dv_z$ give no contribution)

$$\frac{\delta n(\nu)}{n(\nu)} = \tau \frac{x e^x}{e^x - 1} \left\{ \frac{V}{c}\mu + \left(\frac{V}{c}\right)^2 \left[ -1 - \mu^2 + \frac{3 + 11\mu^2}{20} x \coth(x/2) \right] \right.$$
$$+ \frac{kT_e}{m_e c^2}(-4 + x\coth(x/2))$$
$$+ \frac{V}{c}\frac{kT_e}{m_e c^2}\mu \left[ 10 - \frac{47}{5} x \coth(x/2) + \frac{7}{10} x^2 \left( 2\coth^2(x/2) + \frac{1}{\sinh^2(x/2)} \right) \right]$$
$$+ \left(\frac{kT_e}{m_e c^2}\right)^2 \left[ -10 + \frac{47}{2} x \coth(x/2) - \frac{42}{5} x^2 \coth^2(x/2) + \frac{7}{10} x^3 \coth^3(x/2) \right.$$
$$\left. \left. + \frac{7x^2}{5\sinh^2(x/2)}(-3 + x\coth(x/2)) \right] \right\}, \qquad (25)$$

When writing out this equation, we replaced the time integral $\int N_e \sigma_{\rm T} c \, dt$ by the integral taken along the line of sight $\tau = \int N_e(r)\sigma_{\rm T} \, dr$, which is clearly legitimate in the single-scattering approximation we consider.

In the derived formula (25), the terms follow each other in an order that corresponds to an increasing power of $\beta = V/c$ in equation (21). In the problem with a moving cloud, the total electron velocity which corresponds to the parameter $\beta$ in (21) is the sum of its thermal and peculiar components. The first two terms (of the order of $V/c$ and $(V/c)^2$) describe the linear and quadratic kinematic effects and, as one might expect, are of the same form as the terms that are proportional to $\beta$ and $\beta^2$ in formula (21). They are related to the cluster peculiar motion alone. The third term (of the order of $kT_e/m_e c^2$), like the term of the order $(V/c)^2$, results from integrating the term of the order of $\beta^2$ in relation (21), but it is proportional to the square of the thermal velocity. It is easy to verify that, after averaging over $\mu$, the correction proportional to $(V/c)^2$ is of the same form as the correction of the order of $kT_e/m_e c^2$, if we set $(V/c)^2 = 3kT_e/m_e c^2$. This is natural, because such an averaging, for example, describes the situation with chaotic (turbulent) macro motions of blobs of gas in a cluster of galaxies, which is essentially equivalent to the thermal motion of electrons. The cross term which is proportional to $V/c \times kT_e/m_e c^2$ appears after integrating the term of the order of $\beta^3$ in equation (21). Its origin is related both to the peculiar and thermal motions of the electrons. Finally, the term of the order of $(kT_e/m_e c^2)^2$ (which appears after integrating the terms of the order of $\beta^2$ and $\beta^4$) is the main correction to the thermal effect, for which the same expression has been previously derived in the Fokker-Planck approximation (Stebbins 1997; Itoh et al. 1998; Challinor and Lasenby 1998).

It is important to note that expresion (25) which describes the CMB spectral distortion and the nonrelativistic formulas (1) and (2) do not depend on the redshift $z$ of a specific

cluster. This fact is obvious and is attributable to (see, e.g., Sunyaev and Zel'dovich 1980b) the answer being dependent on the parameter $x = h\nu/kT_R$, while the photon frequency and local temperature of the CMB scale in the same way $\propto (1+z)$; in its turn, the cluster optical depth $\tau$ is independent of $z$ (we consider a cloud of gas with specified $T_e$, $V$, and $\tau$).

From formula (25), we can easily derive a relation that is independent of $x$ which describes the spectral distortion in the Rayleigh–Jeans region (for $x \to 0$):

$$\frac{\delta n(\nu)}{n(\nu)} = \tau \left[ \frac{V}{c}\mu + \left(\frac{V}{c}\right)^2 \frac{\mu^2 - 7}{10} - 2\frac{kT_e}{m_e c^2} - \frac{2}{5}\frac{V}{c}\frac{kT_e}{m_e c^2}\mu + \frac{17}{5}\left(\frac{kT_e}{m_e c^2}\right)^2 \right]. \qquad (26)$$

Formula (25) also simplifies in the limit of large $x$ (in the Wien spectral region):

$$\begin{aligned} \frac{\delta n(\nu)}{n(\nu)} = \tau \frac{x e^x}{e^x - 1} \Bigg\{ & \frac{V}{c}\mu + \left(\frac{V}{c}\right)^2 \left( -1 - \mu^2 + \frac{3 + 11\mu^2}{20} x \right) \\ & + \frac{kT_e}{m_e c^2}(-4 + x) + \frac{V}{c}\frac{kT_e}{m_e c^2}\mu \left( 10 - \frac{47}{5}x + \frac{7}{5}x^2 \right) \\ & + \left(\frac{kT_e}{m_e c^2}\right)^2 \left( -10 + \frac{47}{2}x - \frac{42}{5}x^2 + \frac{7}{10}x^3 \right) \Bigg\}. \end{aligned} \qquad (27)$$

For $x \gtrsim 7$, this expression can be used instead of the initial formula (25).

Using relation (25), we obtained a simple approximate formula for calculating the frequency ($X_0$) at which the total CMB spectral distortion in the direction of a moving galaxy cluster vanishes:

$$X_0 = 3.830 \left[ 1 - 0.30\frac{V_r}{c}\frac{m_e c^2}{kT_e} + 1.1\frac{kT_e}{m_e c^2} + 0.00\left(\frac{V_r}{c}\frac{m_e c^2}{kT_e}\right)^2 - 1.5\frac{V_r}{c} \right]. \qquad (28)$$

In this formula, the term proportional to $kT_e/m_e c^2$ has been known previously (Rephaeli 1995; Itoh et al. 1998; Challinor and Lasenby 1998). The origin of the terms of the order of $V_r/c \times m_e c^2/kT_e$ and $(V_r/c \times m_e c^2/kT_e)^2$ is related to the linear kinematic effect, while the last term contains the contribution from the cross effect. Recall that the sign of $V_r$ is positive when the cluster moves toward the observer. We derived similar relations for the positions ($X_{min}$, $X_{max}$) and values ($(\delta I_\nu)_{min}$, $(\delta T_\nu)_{max}$) of the minimum and maximum of the distortion spectrum, which may also prove to be useful in analyzing experimental data:

$$X_{min} = 2.266 \left[1 - 0.20\frac{V_r}{c}\frac{m_e c^2}{kT_e} - 0.2\frac{kT_e}{m_e c^2} - 0.04\left(\frac{V_r}{c}\frac{m_e c^2}{kT_e}\right)^2 + 0.0\frac{V_r}{c}\right], \tag{29}$$

$$(\delta I_\nu)_{min} = -2.059\,\frac{2(kT_R)^3}{(hc)^2}\frac{kT_e}{m_e c^2}\tau \left[1 - 0.83\frac{V_r}{c}\frac{m_e c^2}{kT_e} - 3.8\frac{kT_e}{m_e c^2} + 0.09\left(\frac{V_r}{c}\frac{m_e c^2}{kT_e}\right)^2 + 3.1\frac{V_r}{c}\right], \tag{30}$$

$$X_{max} = 6.511 \left[1 - 0.09\frac{V_r}{c}\frac{m_e c^2}{kT_e} + 2.6\frac{kT_e}{m_e c^2} - 0.01\left(\frac{V_r}{c}\frac{m_e c^2}{kT_e}\right)^2 + 0.4\frac{V_r}{c}\right], \tag{31}$$

$$(\delta I_\nu)_{max} = 3.390\,\frac{2(kT_R)^3}{(hc)^2}\frac{kT_e}{m_e c^2}\tau \left[1 + 0.40\frac{V_r}{c}\frac{m_e c^2}{kT_e} - 7.3\frac{kT_e}{m_e c^2} + 0.05\left(\frac{V_r}{c}\frac{m_e c^2}{kT_e}\right)^2 + 0.8\frac{V_r}{c}\right]. \tag{32}$$

In conclusion, we can calculate the change in the CMB energy flux in the direction of a cluster ($\delta I = \int \delta I_\nu \, d\nu$) and, using relation (28), the fluxes from the "negative" source, i.e., in the frequency range 0 to $X_0$ ($\delta I_-$), and the "positive"source, i.e., at frequencies above $X_0$ ($\delta I_+$):

$$\delta I = \tau I \left[4\frac{V_r}{c} + 4\frac{kT_e}{m_e c^2} + (7\mu^2 - 1)\left(\frac{V}{c}\right)^2 + 20\frac{V_r}{c}\frac{kT_e}{m_e c^2} + 10\left(\frac{kT_e}{m_e c^2}\right)^2\right], \tag{33}$$

$$\delta I_- = \tau I \left[1.5\frac{V_r}{c} - 1.35\frac{kT_e}{m_e c^2} - 0.4\left(\frac{V_\mathrm{r}}{c}\right)^2\frac{m_e c^2}{kT_e} - 2.4\frac{V_r}{c}\frac{kT_e}{m_e c^2} + 3.3\left(\frac{kT_e}{m_e c^2}\right)^2\right], \tag{34}$$

$$\delta I_+ = \tau I \left[2.5\frac{V_r}{c} + 5.35\frac{kT_e}{m_e c^2} + 0.4\left(\frac{V_\mathrm{r}}{c}\right)^2\frac{m_e c^2}{kT_e} + 22.4\frac{V_r}{c}\frac{kT_e}{m_e c^2} + 6.7\left(\frac{kT_e}{m_e c^2}\right)^2\right], \tag{35}$$

where $I = \sigma_R T_R^4/\pi$, and $\sigma_R$ is the Stefan–Boltzman constant. The terms of order $(V/c)^2$ were omitted in formulas (34) and (35). As our Monte Carlo simulations showed, when calculating the luminosity of a moving cluster with the relativistic effects included, formulas (33)–(35) provide an accuracy better than 98% in the range of values $kT_e/m_e c^2 < 0.04$ and $V/c < 0.01$.

Formula (33) again enables us to carry out an energy test of the calculations. It is easy to verify that the terms proportional to $kT_e/m_e c^2$ and $(kT_e/m_e c^2)^2$ are equivalent to the first

two expansion terms in the relativistic formula that describes the rate of energy transfer from thermal electrons to a radiation field (formula (2.42) in the review of Pozdnyakov et al. (1983)). After integrating the correction of order $(V/c)^2$ over $\mu$, we again arrive at relation (23), which describes the energy tranfer due to the cluster peculiar motion.

Note that, according to formula (33), because of the relativistic effects whose origin is related to the high gas temperature, the rate at which the CMB takes off the energy from the electrons increases (by 8.5% at $kT_e = 17$ keV).

## Conclusions and Obervational Implications

In this paper, we showed that the relativistic corrections related to the high degree of heating of the intracluster gas and to the rapid peculiar motions of clusters change appreciably the magnitude and spectrum of the CMB distortion measured in the direction of galaxy clusters. For this reason, they must be taken into account when analyzing the data from future experiments designed to measure the CMB. We also showed that simple analytical expressions written as series in powers of $kT_e/m_ec^2$ and $V/c$ provide the required accuracy over the entire range of frequencies, except for the far Wien spectral region, in which numerical calculations must be used.

As Korolev et al. (1986) pointed out, at large reshifts, it is easier to detect clusters in the microwave range than in X rays. Indeed, the microwave surface brightness of clusters is independent of $z$ (accordingly, the luminosity increases as $(1+z)^4$), while the X-ray surface brightness decreases as $(1+z)^{-3}\exp\left(-h\nu(1+z)/kT_e\right)$. Distant clusters of galaxies can determine the source counts at submillimeter and millimeter wavelengths. The submillimeter flux from clusters additionally increases because of the relativistic effects. As a result, the probability of detecting a cluster at large $z$ also increases. This is particularly important now, because accurate submillimeter spectroscopic measurements will become feasible even in the first decade of the next century, in particular, in the FIRST and Planck Surveyor experiments.

# REFERENCES


Challinor, A. and Lasenby, A., Astrophys. J., 1998 (in press).

Fabbri, R., Astrophys. Space Sci., 1981, vol. 77, p. 529.

Itoh, N., Kohyama, Y., and Nozawa, S, Astrophys. J., 1998 (in press).

Kompaneets, A.C., JETF, 1957, vol. 4, p. 730.

Korolev, V.A., Sunyaev, R.A., and Yakubtsev L.A., Pis'ma Astron. Zh., 1986, vol. 12, p. 141.

Landau, L.D. and Lifshits, E.M., Theory of Fields, Nauka, 1988.

Loeb A., McKee C.F. and Lahav O., Astrophys. J., 1991, vol. 374, p. 44.

Mather, J., Cheng, E.S., Cottingham, D.A., et al., Astrophys. J., 1994, vol. 420, p. 439.

Pozdnyakov, L.A., Sobol', I.M., and Sunyaev, R.A., Astrophys. Space Phys. Rev., 1983, vol. 2, p. 189.

Rephaeli, Y., Astrophys. J., 1995, vol. 445, p. 33.

Stebbins, A., preprint LANL, astro-ph/9709065, 1997.

Sunyaev, R.A. and Zel'dovich, Ya. B., Comments Astrophys. Space Phys., 1972, vol. 4, p. 173.

Sunyaev, R.A., Pis'ma Astron. Zh., 1980, vol. 6, p. 4.

Sunyaev, R.A. and Zel'dovich, Ya. B., Mon. Not. R. Astron. Soc., 1980a, vol. 190, p. 413.

Sunyaev, R.A. and Zel'dovich, Ya. B., Ann. Rev. Astron. Astrophys., 1980b. vol. 18, p. 537.

Taylor, G.B. and Wright, E.L., Astrophys. J., 1989, vol. 339, p. 619.

Tucker, W., Blanco, P., Rappoport, S., et al., preprint LANL, astro-ph/9801120, 1998.

Wright, E.L., Astrophys. J., 1979, vol. 232, p. 348.

Zel'dovich, Ya. B. and Sunyaev, R.A., Astrophys. Space Sci., 1969, vol. 4, p. 301.

**Table 1.** The relativistic correction to the thermal effect (the sum of the $(kT_e/m_ec^2)^n$, $n = 2, 3...$, terms)

| | $\frac{\delta I_\nu}{I_\nu \tau} \frac{\exp x - 1}{x \exp x}$ | | | | |
|---|---|---|---|---|---|
| $x$ | $kT_e/m_ec^2$ | | | | |
| | 0.005 | 0.010 | 0.015 | 0.020 | 0.025 |
| 0.10 | $0.740 \cdot 10^{-4}$ | $0.299 \cdot 10^{-3}$ | $0.670 \cdot 10^{-3}$ | $0.124 \cdot 10^{-2}$ | $0.193 \cdot 10^{-2}$ |
| 0.30 | $0.619 \cdot 10^{-4}$ | $0.264 \cdot 10^{-3}$ | $0.601 \cdot 10^{-3}$ | $0.119 \cdot 10^{-2}$ | $0.186 \cdot 10^{-2}$ |
| 0.50 | $0.585 \cdot 10^{-4}$ | $0.264 \cdot 10^{-3}$ | $0.611 \cdot 10^{-3}$ | $0.124 \cdot 10^{-2}$ | $0.194 \cdot 10^{-2}$ |
| 0.70 | $0.610 \cdot 10^{-4}$ | $0.287 \cdot 10^{-3}$ | $0.672 \cdot 10^{-3}$ | $0.135 \cdot 10^{-2}$ | $0.210 \cdot 10^{-2}$ |
| 0.90 | $0.670 \cdot 10^{-4}$ | $0.324 \cdot 10^{-3}$ | $0.759 \cdot 10^{-3}$ | $0.148 \cdot 10^{-2}$ | $0.230 \cdot 10^{-2}$ |
| 1.10 | $0.747 \cdot 10^{-4}$ | $0.365 \cdot 10^{-3}$ | $0.853 \cdot 10^{-3}$ | $0.162 \cdot 10^{-2}$ | $0.250 \cdot 10^{-2}$ |
| 1.30 | $0.825 \cdot 10^{-4}$ | $0.404 \cdot 10^{-3}$ | $0.940 \cdot 10^{-3}$ | $0.173 \cdot 10^{-2}$ | $0.267 \cdot 10^{-2}$ |
| 1.50 | $0.889 \cdot 10^{-4}$ | $0.436 \cdot 10^{-3}$ | $0.101 \cdot 10^{-2}$ | $0.181 \cdot 10^{-2}$ | $0.279 \cdot 10^{-2}$ |
| 1.70 | $0.931 \cdot 10^{-4}$ | $0.457 \cdot 10^{-3}$ | $0.105 \cdot 10^{-2}$ | $0.185 \cdot 10^{-2}$ | $0.284 \cdot 10^{-2}$ |
| 1.90 | $0.943 \cdot 10^{-4}$ | $0.463 \cdot 10^{-3}$ | $0.105 \cdot 10^{-2}$ | $0.183 \cdot 10^{-2}$ | $0.280 \cdot 10^{-2}$ |
| 2.10 | $0.919 \cdot 10^{-4}$ | $0.453 \cdot 10^{-3}$ | $0.102 \cdot 10^{-2}$ | $0.175 \cdot 10^{-2}$ | $0.267 \cdot 10^{-2}$ |
| 2.30 | $0.855 \cdot 10^{-4}$ | $0.424 \cdot 10^{-3}$ | $0.943 \cdot 10^{-3}$ | $0.160 \cdot 10^{-2}$ | $0.245 \cdot 10^{-2}$ |
| 2.50 | $0.750 \cdot 10^{-4}$ | $0.378 \cdot 10^{-3}$ | $0.829 \cdot 10^{-3}$ | $0.140 \cdot 10^{-2}$ | $0.214 \cdot 10^{-2}$ |
| 2.70 | $0.603 \cdot 10^{-4}$ | $0.313 \cdot 10^{-3}$ | $0.676 \cdot 10^{-3}$ | $0.113 \cdot 10^{-2}$ | $0.173 \cdot 10^{-2}$ |
| 2.90 | $0.415 \cdot 10^{-4}$ | $0.230 \cdot 10^{-3}$ | $0.486 \cdot 10^{-3}$ | $0.805 \cdot 10^{-3}$ | $0.124 \cdot 10^{-2}$ |
| 3.10 | $0.187 \cdot 10^{-4}$ | $0.131 \cdot 10^{-3}$ | $0.262 \cdot 10^{-3}$ | $0.426 \cdot 10^{-3}$ | $0.670 \cdot 10^{-3}$ |
| 3.30 | $-0.777 \cdot 10^{-5}$ | $0.175 \cdot 10^{-4}$ | $0.751 \cdot 10^{-5}$ | $-0.722 \cdot 10^{-6}$ | $0.276 \cdot 10^{-4}$ |
| 3.50 | $-0.375 \cdot 10^{-4}$ | $-0.109 \cdot 10^{-3}$ | $-0.272 \cdot 10^{-3}$ | $-0.469 \cdot 10^{-3}$ | $-0.677 \cdot 10^{-3}$ |
| 3.70 | $-0.702 \cdot 10^{-4}$ | $-0.247 \cdot 10^{-3}$ | $-0.573 \cdot 10^{-3}$ | $-0.972 \cdot 10^{-3}$ | $-0.143 \cdot 10^{-2}$ |
| 3.90 | $-0.105 \cdot 10^{-3}$ | $-0.394 \cdot 10^{-3}$ | $-0.890 \cdot 10^{-3}$ | $-0.150 \cdot 10^{-2}$ | $-0.223 \cdot 10^{-2}$ |
| 4.30 | $-0.180 \cdot 10^{-3}$ | $-0.702 \cdot 10^{-3}$ | $-0.155 \cdot 10^{-2}$ | $-0.261 \cdot 10^{-2}$ | $-0.389 \cdot 10^{-2}$ |
| 4.70 | $-0.257 \cdot 10^{-3}$ | $-0.101 \cdot 10^{-2}$ | $-0.220 \cdot 10^{-2}$ | $-0.371 \cdot 10^{-2}$ | $-0.556 \cdot 10^{-2}$ |
| 5.10 | $-0.330 \cdot 10^{-3}$ | $-0.130 \cdot 10^{-2}$ | $-0.280 \cdot 10^{-2}$ | $-0.474 \cdot 10^{-2}$ | $-0.712 \cdot 10^{-2}$ |
| 5.50 | $-0.393 \cdot 10^{-3}$ | $-0.155 \cdot 10^{-2}$ | $-0.331 \cdot 10^{-2}$ | $-0.561 \cdot 10^{-2}$ | $-0.847 \cdot 10^{-2}$ |
| 5.90 | $-0.439 \cdot 10^{-3}$ | $-0.172 \cdot 10^{-2}$ | $-0.366 \cdot 10^{-2}$ | $-0.626 \cdot 10^{-2}$ | $-0.949 \cdot 10^{-2}$ |
| 6.10 | $-0.453 \cdot 10^{-3}$ | $-0.177 \cdot 10^{-2}$ | $-0.377 \cdot 10^{-2}$ | $-0.647 \cdot 10^{-2}$ | $-0.984 \cdot 10^{-2}$ |
| 6.50 | $-0.461 \cdot 10^{-3}$ | $-0.179 \cdot 10^{-2}$ | $-0.382 \cdot 10^{-2}$ | $-0.661 \cdot 10^{-2}$ | $-0.101 \cdot 10^{-1}$ |
| 6.90 | $-0.433 \cdot 10^{-3}$ | $-0.168 \cdot 10^{-2}$ | $-0.360 \cdot 10^{-2}$ | $-0.630 \cdot 10^{-2}$ | $-0.979 \cdot 10^{-2}$ |
| 7.30 | $-0.361 \cdot 10^{-3}$ | $-0.140 \cdot 10^{-2}$ | $-0.305 \cdot 10^{-2}$ | $-0.546 \cdot 10^{-2}$ | $-0.865 \cdot 10^{-2}$ |
| 7.70 | $-0.238 \cdot 10^{-3}$ | $-0.932 \cdot 10^{-3}$ | $-0.212 \cdot 10^{-2}$ | $-0.398 \cdot 10^{-2}$ | $-0.657 \cdot 10^{-2}$ |
| 8.10 | $-0.546 \cdot 10^{-4}$ | $-0.245 \cdot 10^{-3}$ | $-0.745 \cdot 10^{-3}$ | $-0.175 \cdot 10^{-2}$ | $-0.337 \cdot 10^{-2}$ |
| 8.50 | $0.197 \cdot 10^{-3}$ | $0.693 \cdot 10^{-3}$ | $0.115 \cdot 10^{-2}$ | $0.135 \cdot 10^{-2}$ | $0.113 \cdot 10^{-2}$ |
| 9.30 | $0.941 \cdot 10^{-3}$ | $0.346 \cdot 10^{-2}$ | $0.684 \cdot 10^{-2}$ | $0.108 \cdot 10^{-1}$ | $0.150 \cdot 10^{-1}$ |
| 10.10 | $0.206 \cdot 10^{-2}$ | $0.768 \cdot 10^{-2}$ | $0.157 \cdot 10^{-1}$ | $0.256 \cdot 10^{-1}$ | $0.372 \cdot 10^{-1}$ |
| 10.90 | $0.363 \cdot 10^{-2}$ | $0.137 \cdot 10^{-1}$ | $0.288 \cdot 10^{-1}$ | $0.478 \cdot 10^{-1}$ | $0.707 \cdot 10^{-1}$ |
| 11.70 | $0.571 \cdot 10^{-2}$ | $0.221 \cdot 10^{-1}$ | $0.473 \cdot 10^{-1}$ | $0.799 \cdot 10^{-1}$ | $0.120 \cdot 10^{+0}$ |
| 12.50 | $0.838 \cdot 10^{-2}$ | $0.333 \cdot 10^{-1}$ | $0.730 \cdot 10^{-1}$ | $0.125 \cdot 10^{+0}$ | $0.190 \cdot 10^{+0}$ |
| 13.30 | $0.117 \cdot 10^{-1}$ | $0.481 \cdot 10^{-1}$ | $0.108 \cdot 10^{+0}$ | $0.189 \cdot 10^{+0}$ | $0.290 \cdot 10^{+0}$ |
| 14.10 | $0.159 \cdot 10^{-1}$ | $0.676 \cdot 10^{-1}$ | $0.155 \cdot 10^{+0}$ | $0.277 \cdot 10^{+0}$ | $0.431 \cdot 10^{+0}$ |
| 14.90 | $0.210 \cdot 10^{-1}$ | $0.928 \cdot 10^{-1}$ | $0.218 \cdot 10^{+0}$ | $0.398 \cdot 10^{+0}$ | $0.631 \cdot 10^{+0}$ |
| 15.70 | $0.275 \cdot 10^{-1}$ | $0.126 \cdot 10^{+0}$ | $0.302 \cdot 10^{+0}$ | $0.565 \cdot 10^{+0}$ | $0.913 \cdot 10^{+0}$ |
| 16.50 | $0.357 \cdot 10^{-1}$ | $0.168 \cdot 10^{+0}$ | $0.414 \cdot 10^{+0}$ | $0.794 \cdot 10^{+0}$ | $0.131 \cdot 10^{+1}$ |
| 17.30 | $0.466 \cdot 10^{-1}$ | $0.223 \cdot 10^{+0}$ | $0.565 \cdot 10^{+0}$ | $0.111 \cdot 10^{+1}$ | $0.187 \cdot 10^{+1}$ |
| 18.10 | $0.612 \cdot 10^{-1}$ | $0.294 \cdot 10^{+0}$ | $0.767 \cdot 10^{+0}$ | $0.154 \cdot 10^{+1}$ | $0.266 \cdot 10^{+1}$ |
| 19.10 | $0.876 \cdot 10^{-1}$ | $0.415 \cdot 10^{+0}$ | $0.112 \cdot 10^{+1}$ | $0.229 \cdot 10^{+1}$ | $0.411 \cdot 10^{+1}$ |
| 19.90 | $0.119 \cdot 10^{+0}$ | $0.546 \cdot 10^{+0}$ | $0.152 \cdot 10^{+1}$ | $0.314 \cdot 10^{+1}$ | $0.578 \cdot 10^{+1}$ |

**Table 1 (end).** The relativistic correction to the thermal effect (the sum of the $(kT_e/m_ec^2)^n$, $n = 2, 3...$, terms)

| | $\frac{\delta I_\nu}{I_\nu \tau} \frac{\exp x - 1}{x \exp x}$ | | | | |
|---|---|---|---|---|---|
| $x$ | $kT_e/m_ec^2$ | | | | |
| | 0.030 | 0.035 | 0.040 | 0.045 | 0.050 |
| 0.10 | $0.276 \cdot 10^{-2}$ | $0.368 \cdot 10^{-2}$ | $0.482 \cdot 10^{-2}$ | $0.608 \cdot 10^{-2}$ | $0.744 \cdot 10^{-2}$ |
| 0.30 | $0.267 \cdot 10^{-2}$ | $0.353 \cdot 10^{-2}$ | $0.468 \cdot 10^{-2}$ | $0.594 \cdot 10^{-2}$ | $0.724 \cdot 10^{-2}$ |
| 0.50 | $0.279 \cdot 10^{-2}$ | $0.368 \cdot 10^{-2}$ | $0.490 \cdot 10^{-2}$ | $0.623 \cdot 10^{-2}$ | $0.758 \cdot 10^{-2}$ |
| 0.70 | $0.302 \cdot 10^{-2}$ | $0.401 \cdot 10^{-2}$ | $0.532 \cdot 10^{-2}$ | $0.675 \cdot 10^{-2}$ | $0.820 \cdot 10^{-2}$ |
| 0.90 | $0.330 \cdot 10^{-2}$ | $0.442 \cdot 10^{-2}$ | $0.582 \cdot 10^{-2}$ | $0.736 \cdot 10^{-2}$ | $0.893 \cdot 10^{-2}$ |
| 1.10 | $0.358 \cdot 10^{-2}$ | $0.482 \cdot 10^{-2}$ | $0.630 \cdot 10^{-2}$ | $0.793 \cdot 10^{-2}$ | $0.962 \cdot 10^{-2}$ |
| 1.30 | $0.382 \cdot 10^{-2}$ | $0.515 \cdot 10^{-2}$ | $0.669 \cdot 10^{-2}$ | $0.839 \cdot 10^{-2}$ | $0.102 \cdot 10^{-1}$ |
| 1.50 | $0.398 \cdot 10^{-2}$ | $0.537 \cdot 10^{-2}$ | $0.694 \cdot 10^{-2}$ | $0.867 \cdot 10^{-2}$ | $0.105 \cdot 10^{-1}$ |
| 1.70 | $0.403 \cdot 10^{-2}$ | $0.544 \cdot 10^{-2}$ | $0.701 \cdot 10^{-2}$ | $0.873 \cdot 10^{-2}$ | $0.106 \cdot 10^{-1}$ |
| 1.90 | $0.397 \cdot 10^{-2}$ | $0.535 \cdot 10^{-2}$ | $0.687 \cdot 10^{-2}$ | $0.853 \cdot 10^{-2}$ | $0.103 \cdot 10^{-1}$ |
| 2.10 | $0.378 \cdot 10^{-2}$ | $0.509 \cdot 10^{-2}$ | $0.651 \cdot 10^{-2}$ | $0.806 \cdot 10^{-2}$ | $0.973 \cdot 10^{-2}$ |
| 2.30 | $0.346 \cdot 10^{-2}$ | $0.465 \cdot 10^{-2}$ | $0.594 \cdot 10^{-2}$ | $0.733 \cdot 10^{-2}$ | $0.884 \cdot 10^{-2}$ |
| 2.50 | $0.301 \cdot 10^{-2}$ | $0.403 \cdot 10^{-2}$ | $0.514 \cdot 10^{-2}$ | $0.634 \cdot 10^{-2}$ | $0.763 \cdot 10^{-2}$ |
| 2.70 | $0.243 \cdot 10^{-2}$ | $0.325 \cdot 10^{-2}$ | $0.414 \cdot 10^{-2}$ | $0.509 \cdot 10^{-2}$ | $0.613 \cdot 10^{-2}$ |
| 2.90 | $0.174 \cdot 10^{-2}$ | $0.231 \cdot 10^{-2}$ | $0.294 \cdot 10^{-2}$ | $0.362 \cdot 10^{-2}$ | $0.435 \cdot 10^{-2}$ |
| 3.10 | $0.936 \cdot 10^{-3}$ | $0.123 \cdot 10^{-2}$ | $0.158 \cdot 10^{-2}$ | $0.194 \cdot 10^{-2}$ | $0.233 \cdot 10^{-2}$ |
| 3.30 | $0.380 \cdot 10^{-4}$ | $0.276 \cdot 10^{-4}$ | $0.543 \cdot 10^{-4}$ | $0.754 \cdot 10^{-4}$ | $0.955 \cdot 10^{-4}$ |
| 3.50 | $-0.943 \cdot 10^{-3}$ | $-0.128 \cdot 10^{-2}$ | $-0.160 \cdot 10^{-2}$ | $-0.194 \cdot 10^{-2}$ | $-0.232 \cdot 10^{-2}$ |
| 3.70 | $-0.199 \cdot 10^{-2}$ | $-0.267 \cdot 10^{-2}$ | $-0.335 \cdot 10^{-2}$ | $-0.408 \cdot 10^{-2}$ | $-0.488 \cdot 10^{-2}$ |
| 3.90 | $-0.309 \cdot 10^{-2}$ | $-0.412 \cdot 10^{-2}$ | $-0.519 \cdot 10^{-2}$ | $-0.632 \cdot 10^{-2}$ | $-0.755 \cdot 10^{-2}$ |
| 4.30 | $-0.539 \cdot 10^{-2}$ | $-0.713 \cdot 10^{-2}$ | $-0.899 \cdot 10^{-2}$ | $-0.110 \cdot 10^{-1}$ | $-0.131 \cdot 10^{-1}$ |
| 4.70 | $-0.769 \cdot 10^{-2}$ | $-0.101 \cdot 10^{-1}$ | $-0.128 \cdot 10^{-1}$ | $-0.156 \cdot 10^{-1}$ | $-0.186 \cdot 10^{-1}$ |
| 5.10 | $-0.986 \cdot 10^{-2}$ | $-0.130 \cdot 10^{-1}$ | $-0.164 \cdot 10^{-1}$ | $-0.200 \cdot 10^{-1}$ | $-0.239 \cdot 10^{-1}$ |
| 5.50 | $-0.118 \cdot 10^{-1}$ | $-0.154 \cdot 10^{-1}$ | $-0.196 \cdot 10^{-1}$ | $-0.239 \cdot 10^{-1}$ | $-0.286 \cdot 10^{-1}$ |
| 5.90 | $-0.132 \cdot 10^{-1}$ | $-0.174 \cdot 10^{-1}$ | $-0.221 \cdot 10^{-1}$ | $-0.271 \cdot 10^{-1}$ | $-0.325 \cdot 10^{-1}$ |
| 6.10 | $-0.137 \cdot 10^{-1}$ | $-0.181 \cdot 10^{-1}$ | $-0.230 \cdot 10^{-1}$ | $-0.283 \cdot 10^{-1}$ | $-0.340 \cdot 10^{-1}$ |
| 6.50 | $-0.142 \cdot 10^{-1}$ | $-0.188 \cdot 10^{-1}$ | $-0.241 \cdot 10^{-1}$ | $-0.297 \cdot 10^{-1}$ | $-0.359 \cdot 10^{-1}$ |
| 6.90 | $-0.139 \cdot 10^{-1}$ | $-0.185 \cdot 10^{-1}$ | $-0.239 \cdot 10^{-1}$ | $-0.297 \cdot 10^{-1}$ | $-0.361 \cdot 10^{-1}$ |
| 7.30 | $-0.125 \cdot 10^{-1}$ | $-0.169 \cdot 10^{-1}$ | $-0.220 \cdot 10^{-1}$ | $-0.277 \cdot 10^{-1}$ | $-0.340 \cdot 10^{-1}$ |
| 7.70 | $-0.982 \cdot 10^{-2}$ | $-0.137 \cdot 10^{-1}$ | $-0.182 \cdot 10^{-1}$ | $-0.234 \cdot 10^{-1}$ | $-0.292 \cdot 10^{-1}$ |
| 8.10 | $-0.564 \cdot 10^{-2}$ | $-0.855 \cdot 10^{-2}$ | $-0.120 \cdot 10^{-1}$ | $-0.163 \cdot 10^{-1}$ | $-0.211 \cdot 10^{-1}$ |
| 8.50 | $0.312 \cdot 10^{-3}$ | $-0.110 \cdot 10^{-2}$ | $-0.298 \cdot 10^{-2}$ | $-0.574 \cdot 10^{-2}$ | $-0.896 \cdot 10^{-2}$ |
| 9.30 | $0.189 \cdot 10^{-1}$ | $0.225 \cdot 10^{-1}$ | $0.259 \cdot 10^{-1}$ | $0.285 \cdot 10^{-1}$ | $0.309 \cdot 10^{-1}$ |
| 10.10 | $0.492 \cdot 10^{-1}$ | $0.616 \cdot 10^{-1}$ | $0.742 \cdot 10^{-1}$ | $0.863 \cdot 10^{-1}$ | $0.988 \cdot 10^{-1}$ |
| 10.90 | $0.955 \cdot 10^{-1}$ | $0.122 \cdot 10^{+0}$ | $0.150 \cdot 10^{+0}$ | $0.178 \cdot 10^{+0}$ | $0.207 \cdot 10^{+0}$ |
| 11.70 | $0.164 \cdot 10^{+0}$ | $0.213 \cdot 10^{+0}$ | $0.265 \cdot 10^{+0}$ | $0.318 \cdot 10^{+0}$ | $0.374 \cdot 10^{+0}$ |
| 12.50 | $0.264 \cdot 10^{+0}$ | $0.347 \cdot 10^{+0}$ | $0.436 \cdot 10^{+0}$ | $0.530 \cdot 10^{+0}$ | $0.629 \cdot 10^{+0}$ |
| 13.30 | $0.409 \cdot 10^{+0}$ | $0.543 \cdot 10^{+0}$ | $0.691 \cdot 10^{+0}$ | $0.849 \cdot 10^{+0}$ | $0.102 \cdot 10^{+1}$ |
| 14.10 | $0.617 \cdot 10^{+0}$ | $0.830 \cdot 10^{+0}$ | $0.107 \cdot 10^{+1}$ | $0.133 \cdot 10^{+1}$ | $0.161 \cdot 10^{+1}$ |
| 14.90 | $0.917 \cdot 10^{+0}$ | $0.125 \cdot 10^{+1}$ | $0.164 \cdot 10^{+1}$ | $0.205 \cdot 10^{+1}$ | $0.251 \cdot 10^{+1}$ |
| 15.70 | $0.135 \cdot 10^{+1}$ | $0.187 \cdot 10^{+1}$ | $0.248 \cdot 10^{+1}$ | $0.315 \cdot 10^{+1}$ | $0.390 \cdot 10^{+1}$ |
| 16.50 | $0.197 \cdot 10^{+1}$ | $0.278 \cdot 10^{+1}$ | $0.374 \cdot 10^{+1}$ | $0.481 \cdot 10^{+1}$ | $0.603 \cdot 10^{+1}$ |
| 17.30 | $0.287 \cdot 10^{+1}$ | $0.413 \cdot 10^{+1}$ | $0.561 \cdot 10^{+1}$ | $0.730 \cdot 10^{+1}$ | $0.926 \cdot 10^{+1}$ |
| 18.10 | $0.416 \cdot 10^{+1}$ | $0.610 \cdot 10^{+1}$ | $0.838 \cdot 10^{+1}$ | $0.110 \cdot 10^{+2}$ | $0.141 \cdot 10^{+2}$ |
| 19.10 | $0.657 \cdot 10^{+1}$ | $0.988 \cdot 10^{+1}$ | $0.137 \cdot 10^{+2}$ | $0.182 \cdot 10^{+2}$ | $0.237 \cdot 10^{+2}$ |
| 19.90 | $0.940 \cdot 10^{+1}$ | $0.144 \cdot 10^{+2}$ | $0.202 \cdot 10^{+2}$ | $0.269 \cdot 10^{+2}$ | $0.354 \cdot 10^{+2}$ |

**Table 2.** The "cross" relativistic correction
(the sum of the $V_r/c \times (kT_e/m_ec^2)^n$, $n = 1, 2...$, terms)

| | $\frac{\delta I_\nu}{I_\nu(V_r/c)\tau} \frac{\exp x - 1}{x \exp x}$ | | | | |
|---|---|---|---|---|---|
| $x$ | $kT_e/m_ec^2$ | | | | |
| | 0.01 | 0.02 | 0.03 | 0.04 | 0.05 |
| 0.20 | -0.334·10$^{-2}$ | -0.629·10$^{-2}$ | -0.139·10$^{-1}$ | -0.232·10$^{-1}$ | -0.343·10$^{-1}$ |
| 0.60 | -0.586·10$^{-2}$ | -0.109·10$^{-1}$ | -0.248·10$^{-1}$ | -0.435·10$^{-1}$ | -0.642·10$^{-1}$ |
| 1.00 | -0.114·10$^{-1}$ | -0.209·10$^{-1}$ | -0.384·10$^{-1}$ | -0.621·10$^{-1}$ | -0.851·10$^{-1}$ |
| 1.40 | -0.185·10$^{-1}$ | -0.335·10$^{-1}$ | -0.537·10$^{-1}$ | -0.799·10$^{-1}$ | -0.102·10$^{+0}$ |
| 1.80 | -0.260·10$^{-1}$ | -0.467·10$^{-1}$ | -0.694·10$^{-1}$ | -0.967·10$^{-1}$ | -0.117·10$^{+0}$ |
| 2.20 | -0.328·10$^{-1}$ | -0.587·10$^{-1}$ | -0.841·10$^{-1}$ | -0.112·10$^{+0}$ | -0.131·10$^{+0}$ |
| 2.60 | -0.383·10$^{-1}$ | -0.683·10$^{-1}$ | -0.966·10$^{-1}$ | -0.125·10$^{+0}$ | -0.144·10$^{+0}$ |
| 3.00 | -0.417·10$^{-1}$ | -0.745·10$^{-1}$ | -0.105·10$^{+0}$ | -0.133·10$^{+0}$ | -0.155·10$^{+0}$ |
| 3.40 | -0.426·10$^{-1}$ | -0.764·10$^{-1}$ | -0.109·10$^{+0}$ | -0.137·10$^{+0}$ | -0.160·10$^{+0}$ |
| 3.80 | -0.405·10$^{-1}$ | -0.736·10$^{-1}$ | -0.107·10$^{+0}$ | -0.133·10$^{+0}$ | -0.159·10$^{+0}$ |
| 4.20 | -0.351·10$^{-1}$ | -0.655·10$^{-1}$ | -0.976·10$^{-1}$ | -0.122·10$^{+0}$ | -0.149·10$^{+0}$ |
| 4.60 | -0.263·10$^{-1}$ | -0.517·10$^{-1}$ | -0.800·10$^{-1}$ | -0.101·10$^{+0}$ | -0.127·10$^{+0}$ |
| 5.00 | -0.137·10$^{-1}$ | -0.318·10$^{-1}$ | -0.533·10$^{-1}$ | -0.695·10$^{-1}$ | -0.921·10$^{-1}$ |
| 5.40 | 0.290·10$^{-2}$ | -0.538·10$^{-2}$ | -0.169·10$^{-1}$ | -0.265·10$^{-1}$ | -0.424·10$^{-1}$ |
| 5.80 | 0.236·10$^{-1}$ | 0.282·10$^{-1}$ | 0.302·10$^{-1}$ | 0.291·10$^{-1}$ | 0.234·10$^{-1}$ |
| 6.20 | 0.487·10$^{-1}$ | 0.696·10$^{-1}$ | 0.886·10$^{-1}$ | 0.986·10$^{-1}$ | 0.107·10$^{+0}$ |
| 6.60 | 0.783·10$^{-1}$ | 0.120·10$^{+0}$ | 0.159·10$^{+0}$ | 0.183·10$^{+0}$ | 0.208·10$^{+0}$ |
| 7.00 | 0.113·10$^{+0}$ | 0.180·10$^{+0}$ | 0.244·10$^{+0}$ | 0.285·10$^{+0}$ | 0.330·10$^{+0}$ |
| 7.40 | 0.153·10$^{+0}$ | 0.251·10$^{+0}$ | 0.343·10$^{+0}$ | 0.405·10$^{+0}$ | 0.474·10$^{+0}$ |
| 7.80 | 0.198·10$^{+0}$ | 0.334·10$^{+0}$ | 0.459·10$^{+0}$ | 0.548·10$^{+0}$ | 0.643·10$^{+0}$ |
| 8.20 | 0.250·10$^{+0}$ | 0.433·10$^{+0}$ | 0.595·10$^{+0}$ | 0.716·10$^{+0}$ | 0.840·10$^{+0}$ |
| 8.60 | 0.308·10$^{+0}$ | 0.553·10$^{+0}$ | 0.759·10$^{+0}$ | 0.924·10$^{+0}$ | 0.106·10$^{+1}$ |
| 9.40 | 0.448·10$^{+0}$ | 0.839·10$^{+0}$ | 0.116·10$^{+1}$ | 0.143·10$^{+1}$ | 0.167·10$^{+1}$ |
| 10.20 | 0.624·10$^{+0}$ | 0.123·10$^{+1}$ | 0.172·10$^{+1}$ | 0.219·10$^{+1}$ | 0.255·10$^{+1}$ |
| 11.00 | 0.844·10$^{+0}$ | 0.176·10$^{+1}$ | 0.252·10$^{+1}$ | 0.329·10$^{+1}$ | 0.388·10$^{+1}$ |
| 11.80 | 0.112·10$^{+1}$ | 0.245·10$^{+1}$ | 0.366·10$^{+1}$ | 0.492·10$^{+1}$ | 0.592·10$^{+1}$ |
| 12.60 | 0.146·10$^{+1}$ | 0.336·10$^{+1}$ | 0.529·10$^{+1}$ | 0.734·10$^{+1}$ | 0.906·10$^{+1}$ |
| 13.40 | 0.187·10$^{+1}$ | 0.452·10$^{+1}$ | 0.762·10$^{+1}$ | 0.109·10$^{+2}$ | 0.139·10$^{+2}$ |
| 14.20 | 0.238·10$^{+1}$ | 0.600·10$^{+1}$ | 0.109·10$^{+2}$ | 0.160·10$^{+2}$ | 0.211·10$^{+2}$ |
| 15.00 | 0.300·10$^{+1}$ | 0.783·10$^{+1}$ | 0.155·10$^{+2}$ | 0.233·10$^{+2}$ | 0.317·10$^{+2}$ |
| 15.80 | 0.373·10$^{+1}$ | 0.101·10$^{+2}$ | 0.218·10$^{+2}$ | 0.335·10$^{+2}$ | 0.470·10$^{+2}$ |
| 16.60 | 0.460·10$^{+1}$ | 0.128·10$^{+2}$ | 0.304·10$^{+2}$ | 0.476·10$^{+2}$ | 0.686·10$^{+2}$ |
| 17.40 | 0.562·10$^{+1}$ | 0.161·10$^{+2}$ | 0.419·10$^{+2}$ | 0.666·10$^{+2}$ | 0.985·10$^{+2}$ |
| 18.20 | 0.680·10$^{+1}$ | 0.200·10$^{+2}$ | 0.571·10$^{+2}$ | 0.921·10$^{+2}$ | 0.139·10$^{+3}$ |
| 19.00 | 0.815·10$^{+1}$ | 0.245·10$^{+2}$ | 0.770·10$^{+2}$ | 0.126·10$^{+3}$ | 0.194·10$^{+3}$ |
| 19.80 | 0.967·10$^{+1}$ | 0.297·10$^{+2}$ | 0.103·10$^{+3}$ | 0.169·10$^{+3}$ | 0.266·10$^{+3}$ |

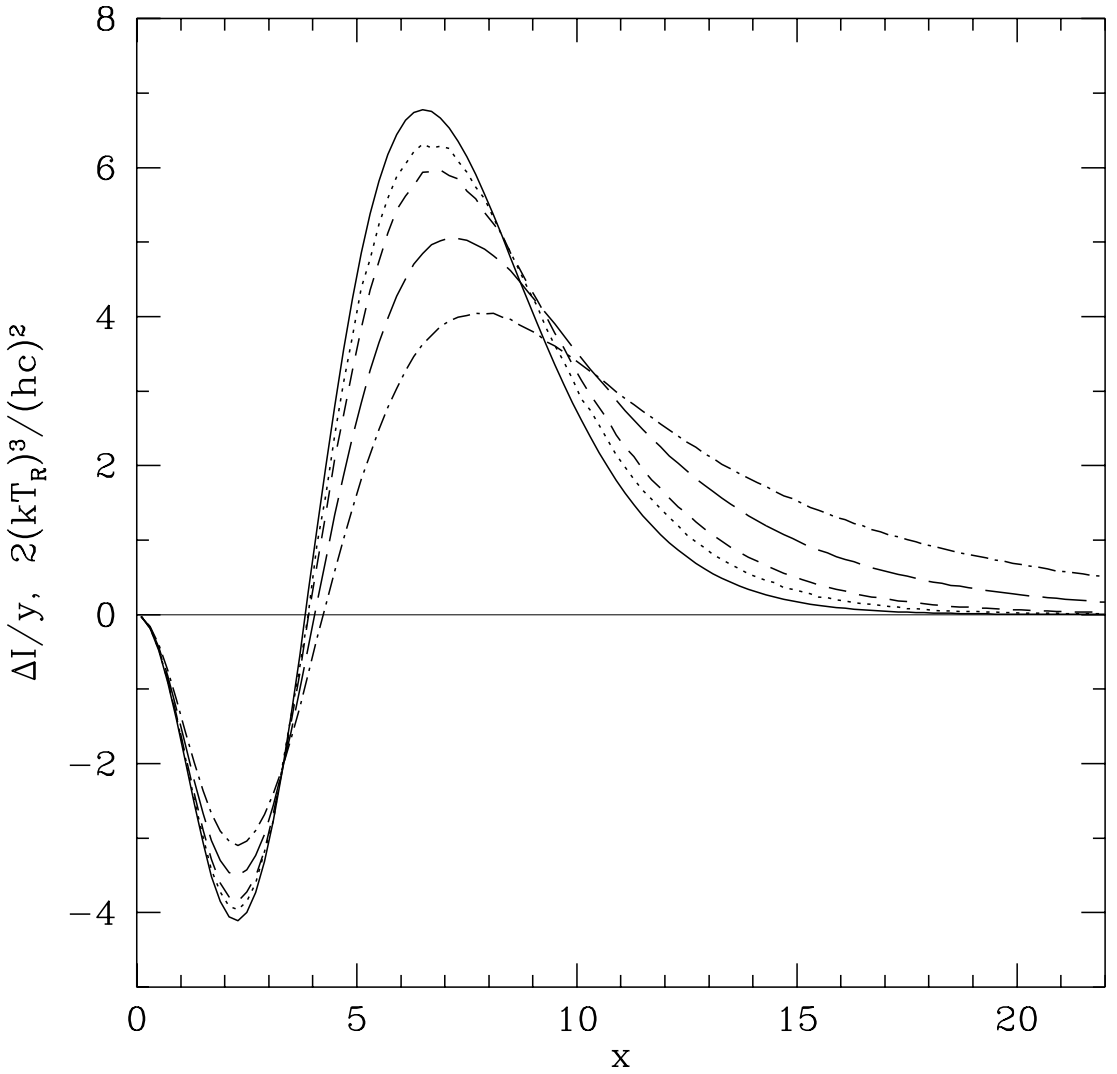


Figure 1: CMB distortion spectra in the direction of an optically thin cloud of thermal electrons calculated by the Monte Carlo method for various temperatures $kT_e/m_ec^2$: 0.01 (dotted line), 0.02 (short dashes), 0.05 (long dashes), 0.1 (dash-dotted line). The solid line indicates the distortion due to the linear effect given by formula (1).

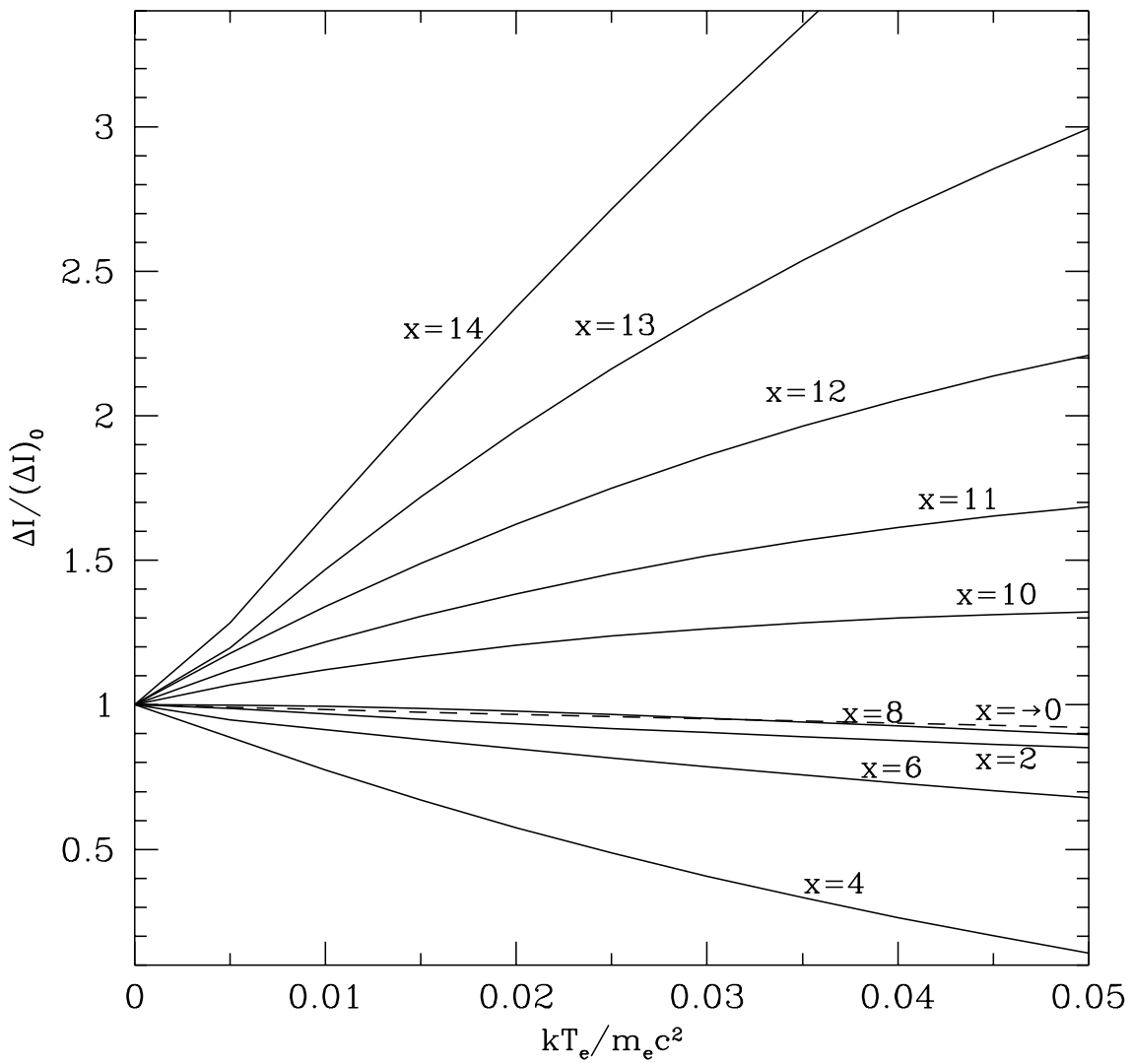


Figure 2: The ratio of the actual spectral distortion to the distortion calculated from formula (1) versus $kT_e/m_ec^2$ for various frequencies $x$, including the Rayleigh-Jeans region ($x \to 0$).

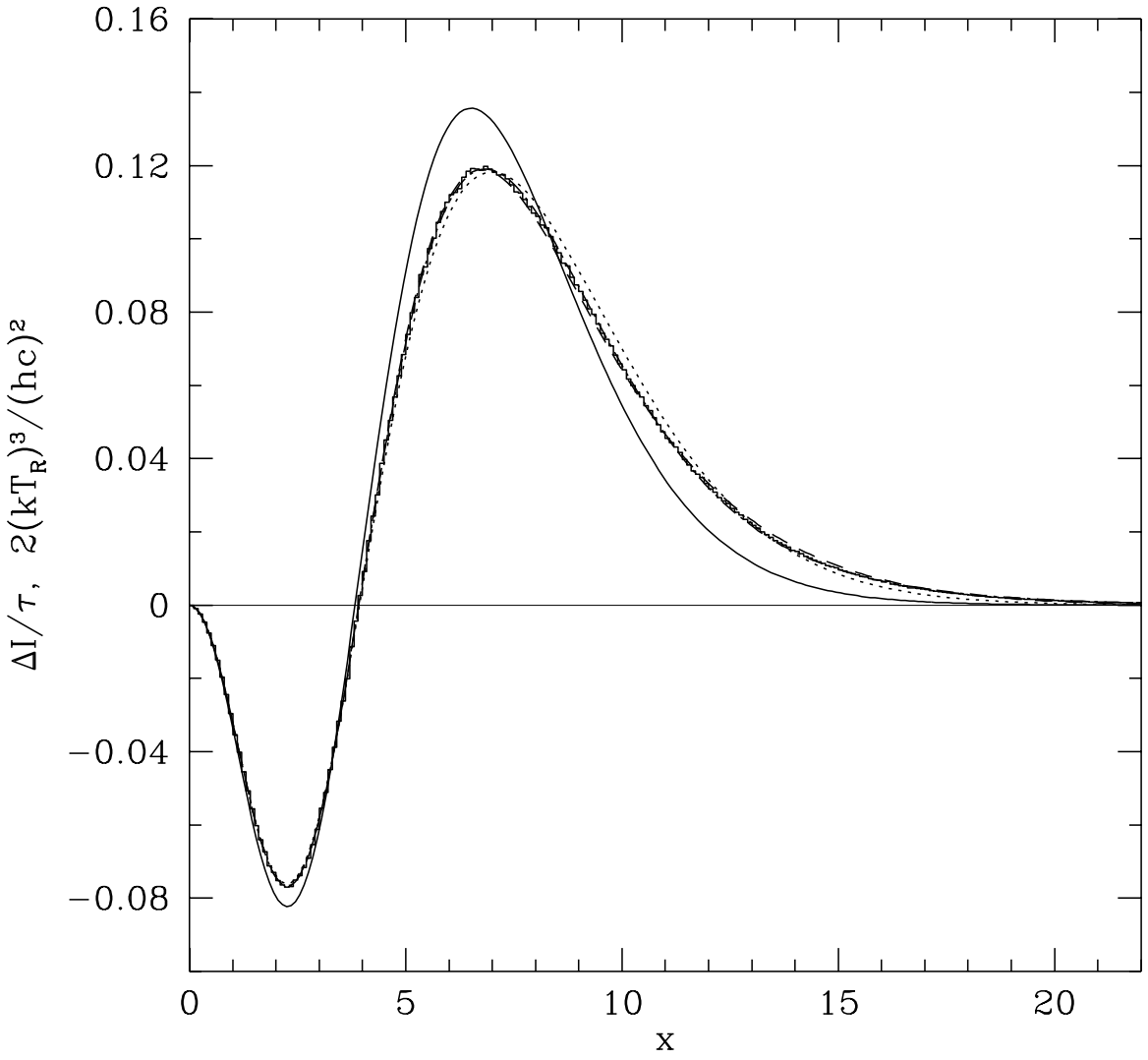


Figure 3: The Monte Carlo spectrum of the thermal effect (histogram) in comparison with the spectrum calculated from the analytical formula (Itoh et al. 1998) with allowance for different numbers of terms of the expansion in $kT_e/m_ec^2$: only the first term (solid line) – described by formula (1), the first two (dotted line), the first three (dashed line), the first four (dash-dotted line). The parameter $kT_e/m_ec^2 = 0.02$.

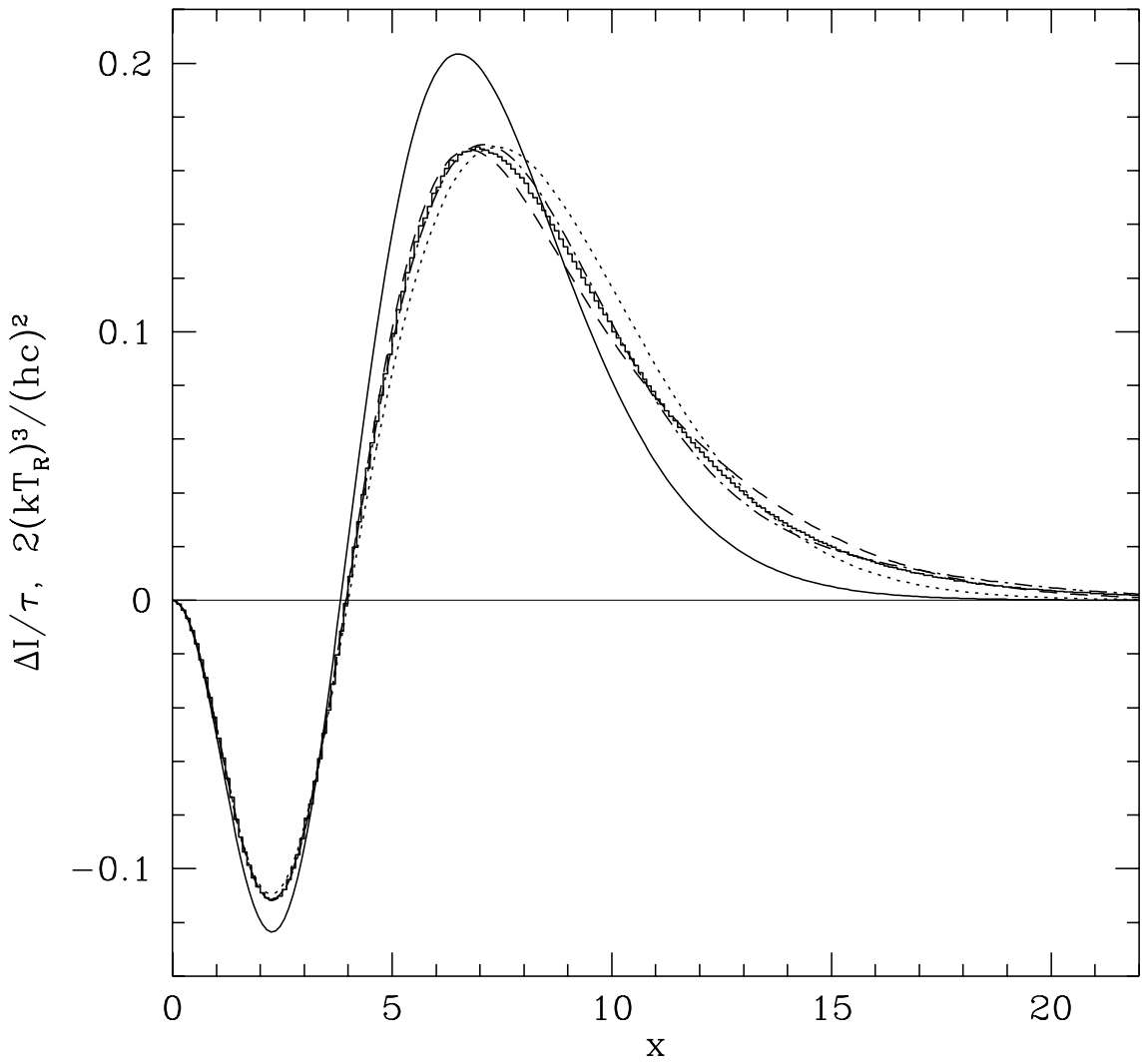


Figure 4: The same as Fig. 3, but for $kT_e/m_ec^2 = 0.03$.

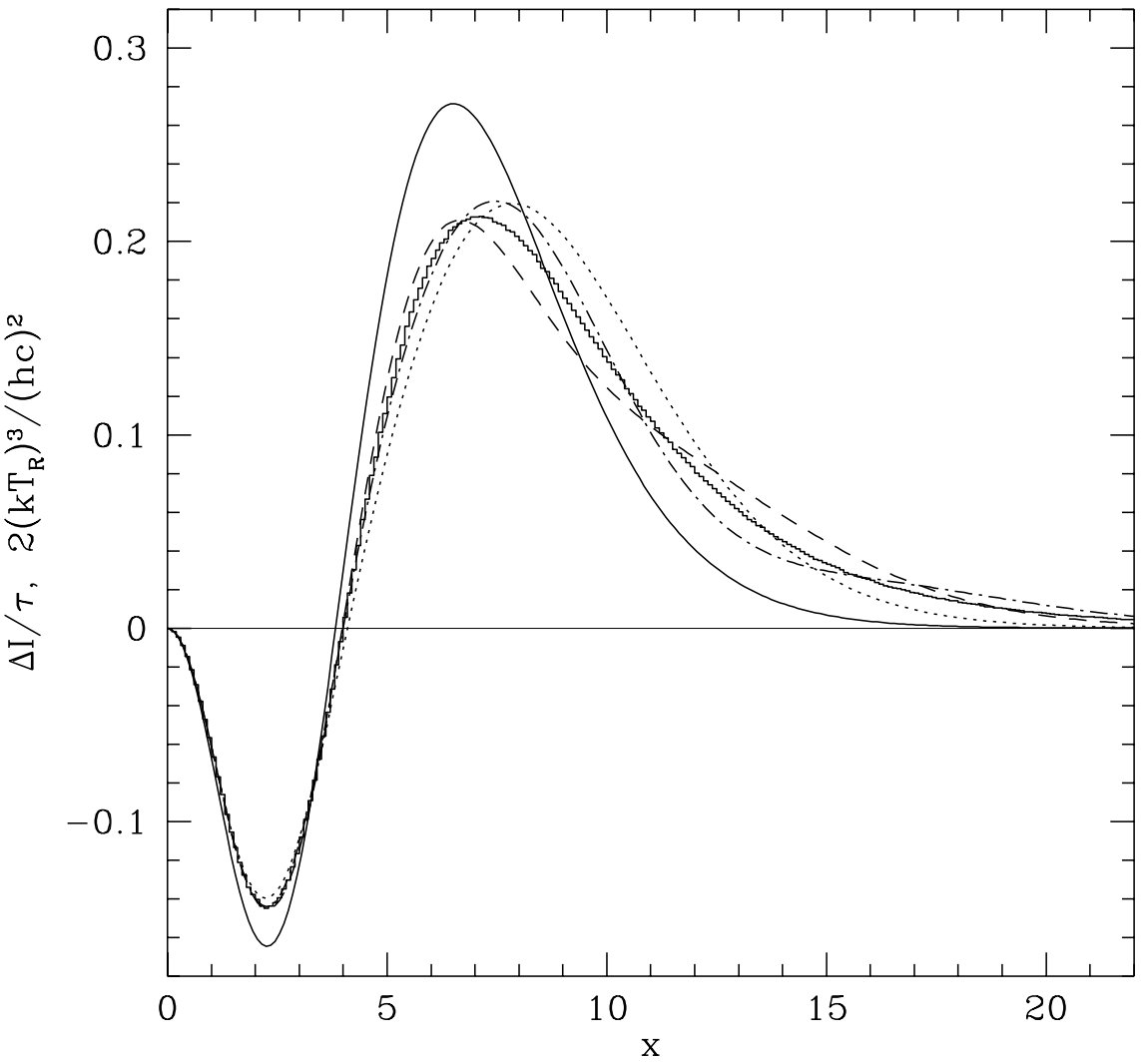


Figure 5: The same as Fig. 3, but ior $kT_e/m_ec^2 = 0.04$.

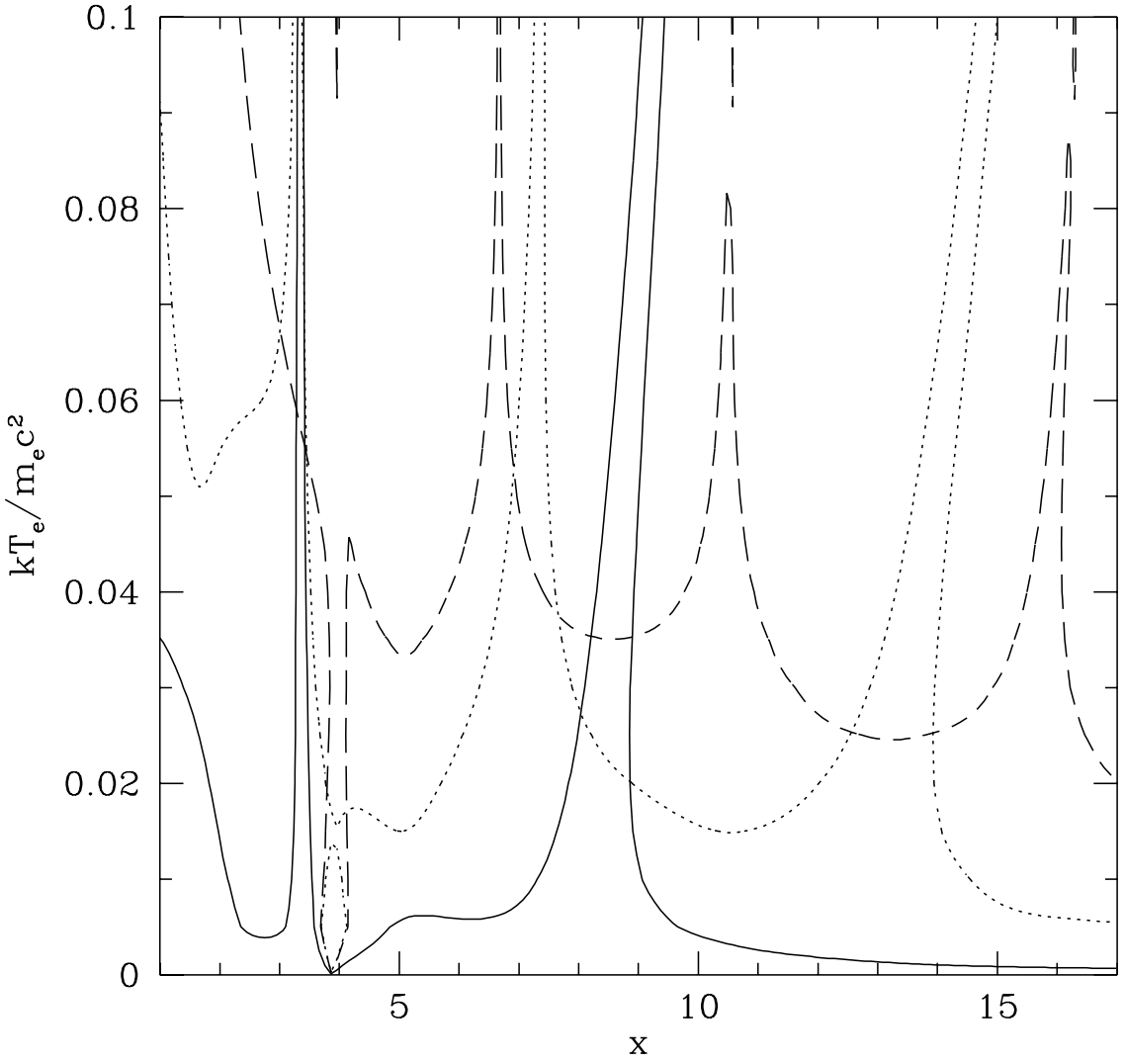


Figure 6: The region within which the error in the calculation of the thermal effect from the analytical formula is no greater than 5%. The formula allows for different numbers of terms of the expansion in $kT_e/mc^2$: formula (1) – the region under the solid line, the first two terms (the region under the dotted line), the first four terms (the region under the dashed line).

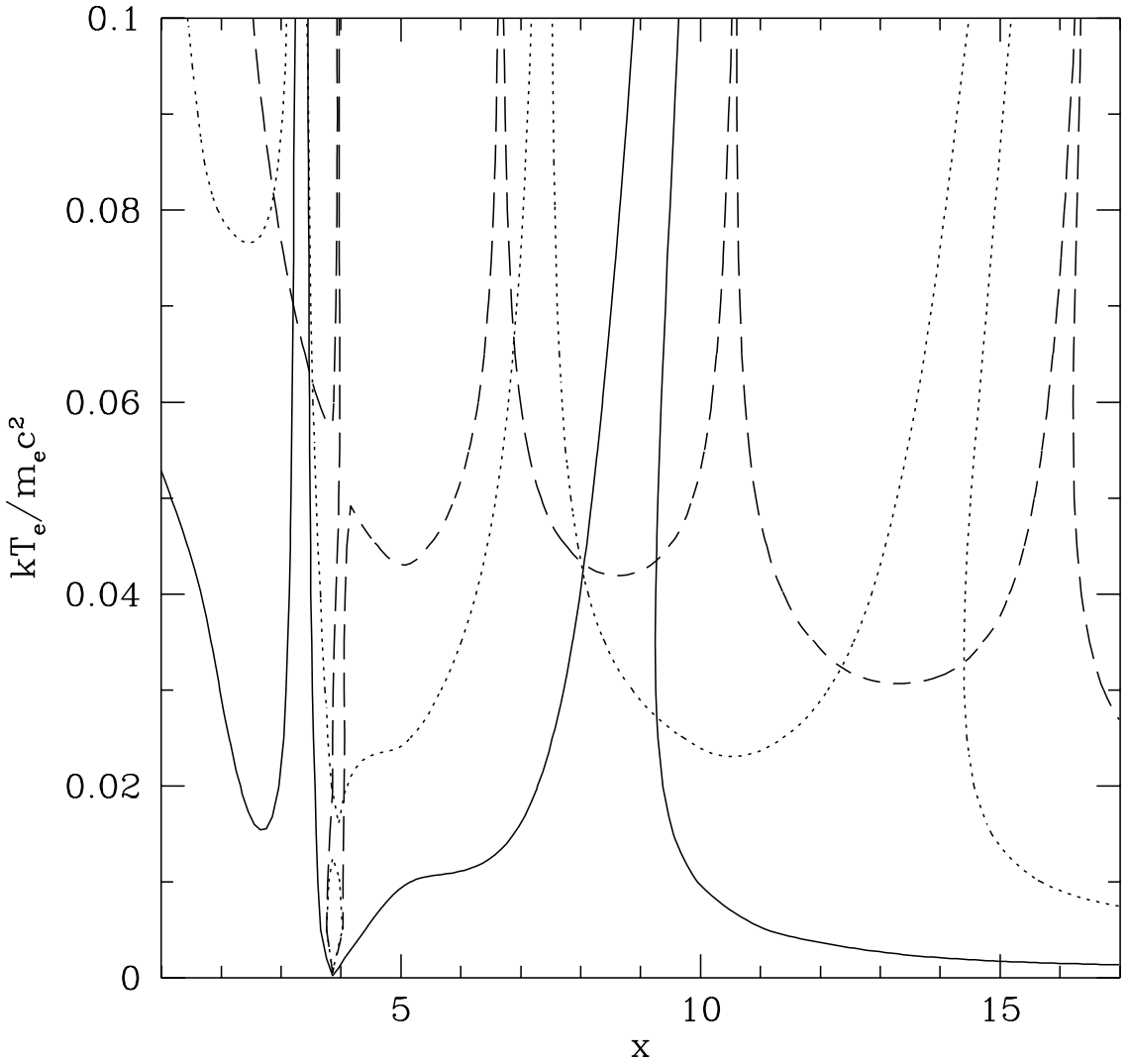


Figure 7: The same as Fig. 6, but for an error of 10%.

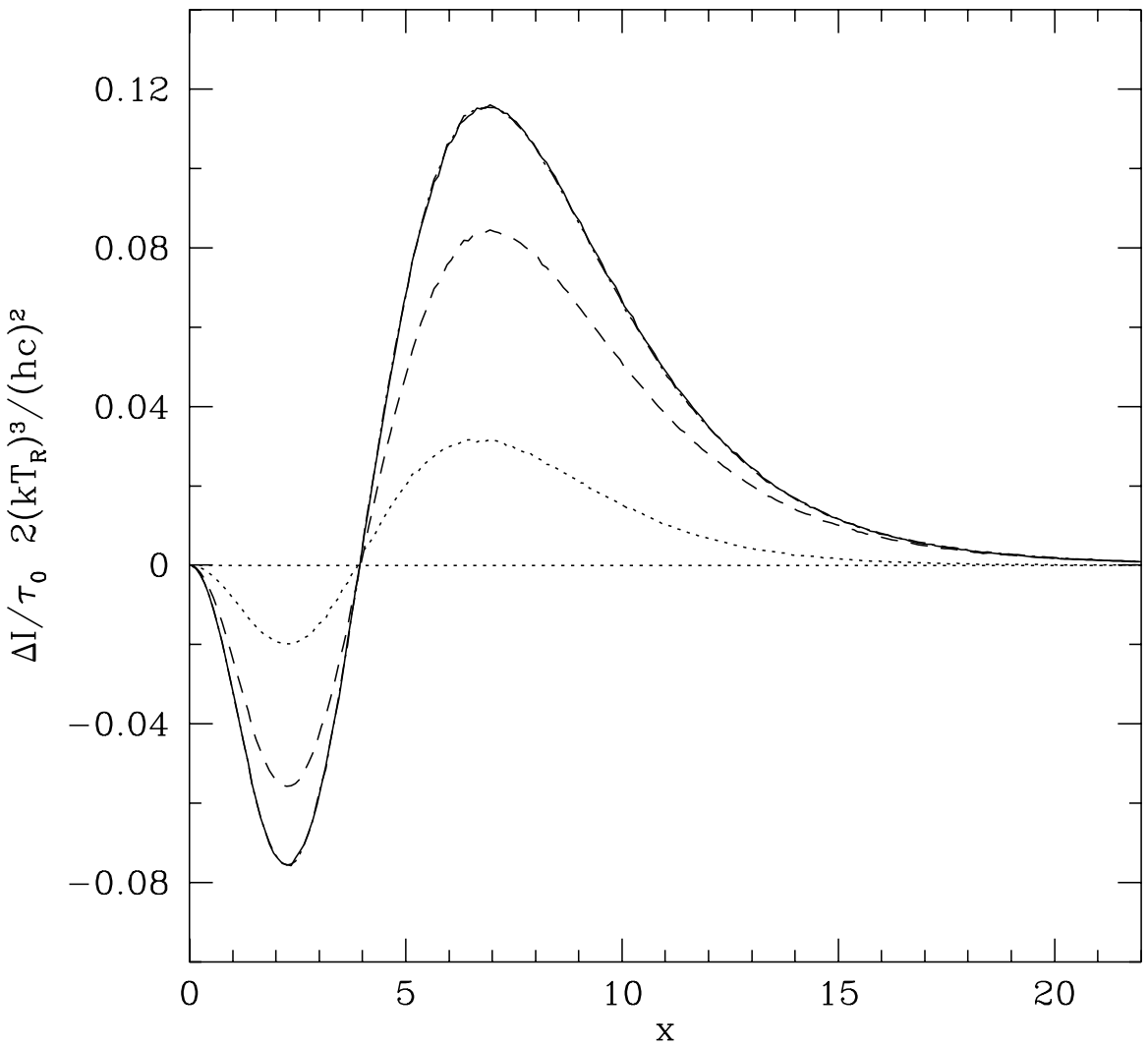


Figure 8: The spectrum of the CMB distortion due to the scattering by a cloud of hot electrons that consists of two layers: one with $kT_e/m_ec^2 = 0.01$ and the other with $kT_e/m_ec^2 = 0.03$. The optical depths of the layers are the same ($\tau_0$). The total distortion is indicated by the solid line; the distortion from the first layer, by the dotted line; and the distortion from the second layer, by the dashed line. A one-component model fit for $kT_e/m_ec^2 = 0.025$ and $\tau = 0.8\tau_0$ is indicated by the dash-dotted line (virtually merges with the solid line). All the spectra were obtained by the Monte Carlo method.

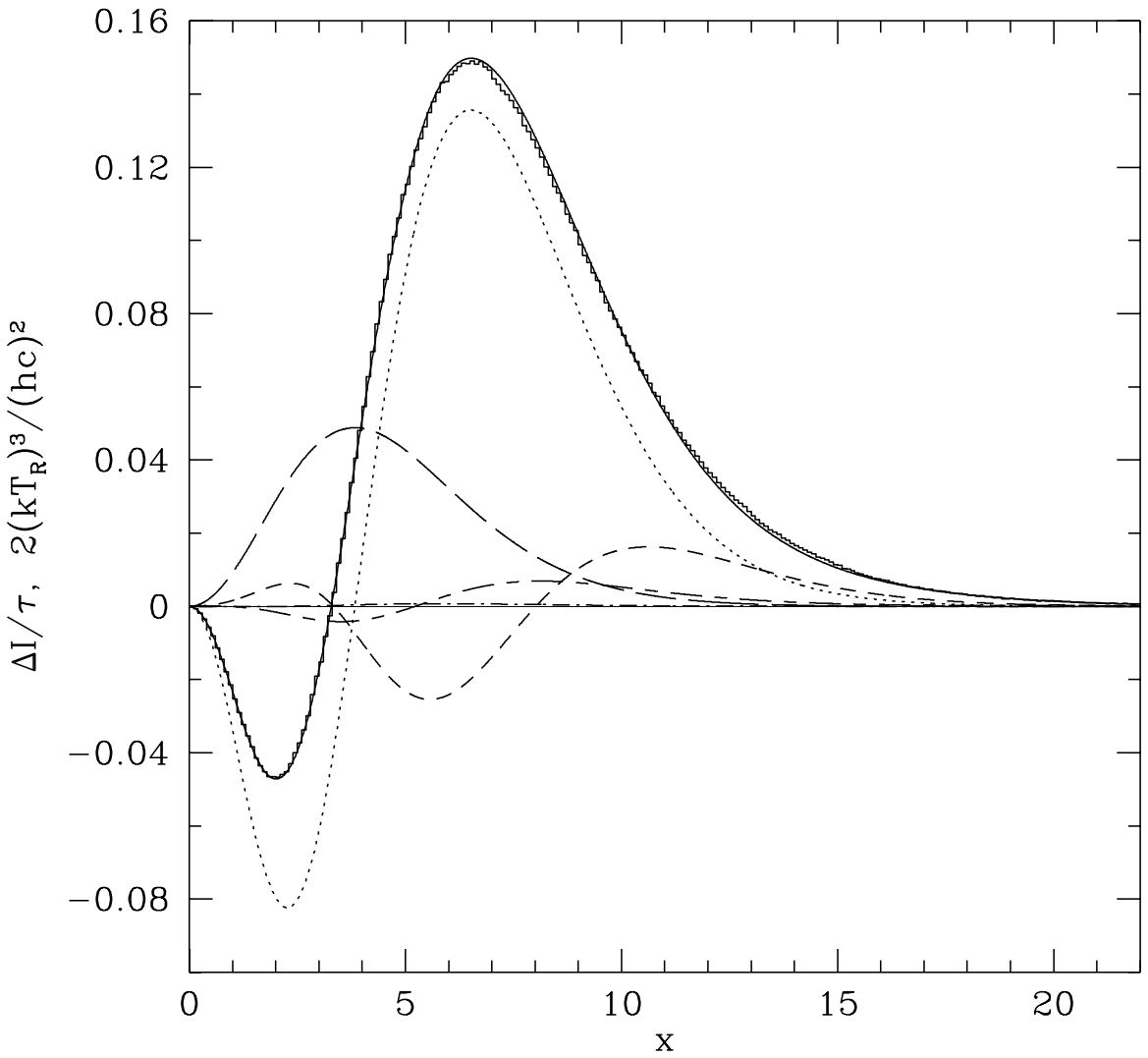


Figure 9: The Monte Carlo spectrum of the CMB distortion in the direction of a moving cluster of galaxies with hot gas (histogram) for the following parameters: $kT_e/m_ec^2 = 0.02$ ($T_e = 10.2$ keV), $V/c = 0.01$ ($V = 3000$ km/s), $\mu = 1$ (the cluster moves toward the observer). The solid line represents the spectrum that was obtained by adding the analytical expressions that describe the thermal and kinematic effects and their first relativistic corrections [we used the results obtained by Itoh et al. (1998) and in this paper]. Also shown are the contributions from individual components: $\propto kT_e/m_ec^2$ (dotted line) – given by formula (1), $\propto (kT_e/m_ec^2)^2$ (short dashes), $\propto V/c$ (long dashes) – given by formula (2), $\propto (V/c)^2$ (dash-dotted line), $\propto V/c \times kT_e/m_ec^2$ (alternating long and short dashes).

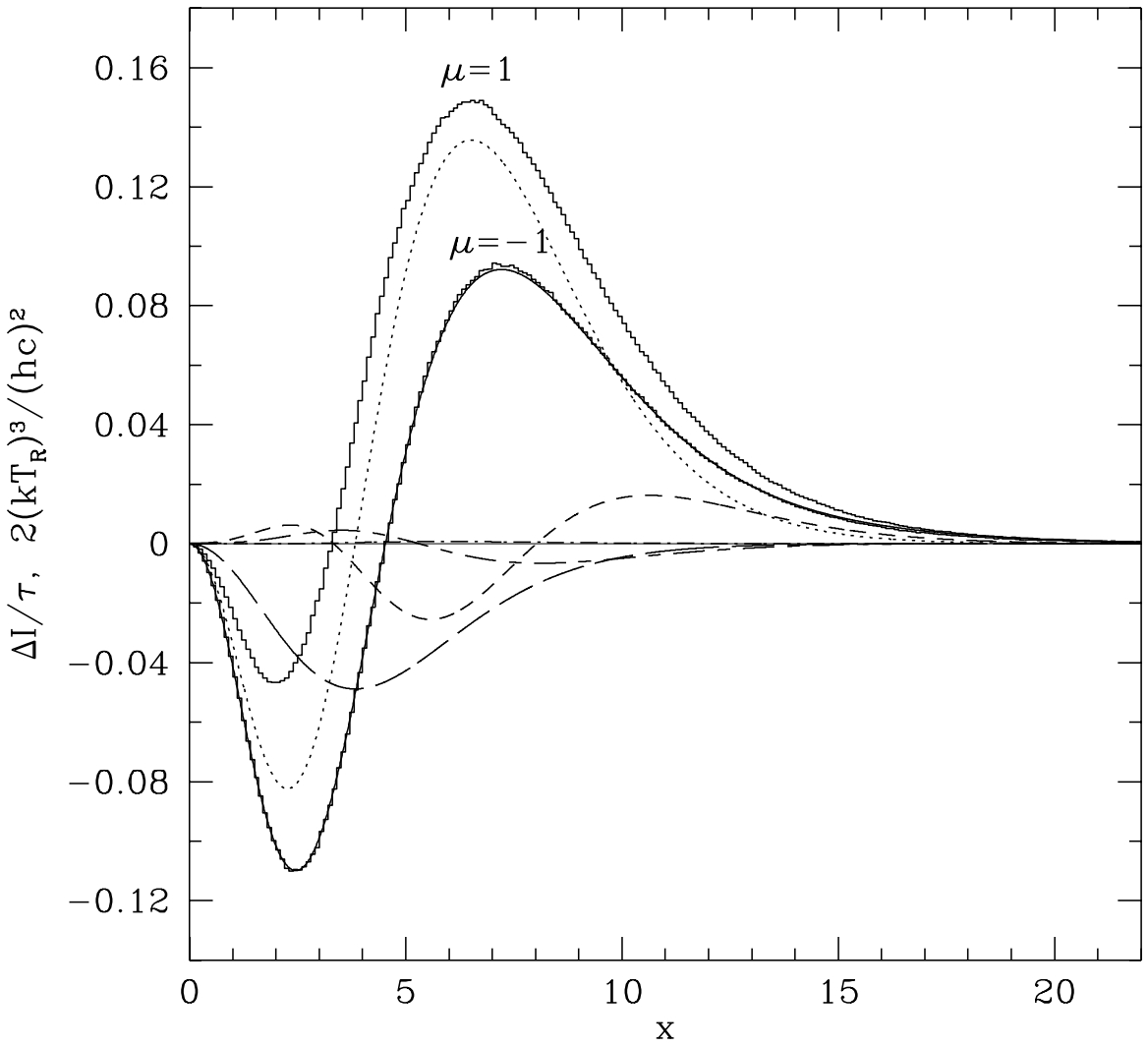


Figure 10: The same as Fig. 9, but for $\mu = -1$ (the cluster moving away from us). For comparison, the distortion spectrum for $\mu = 1$ is reproduced.

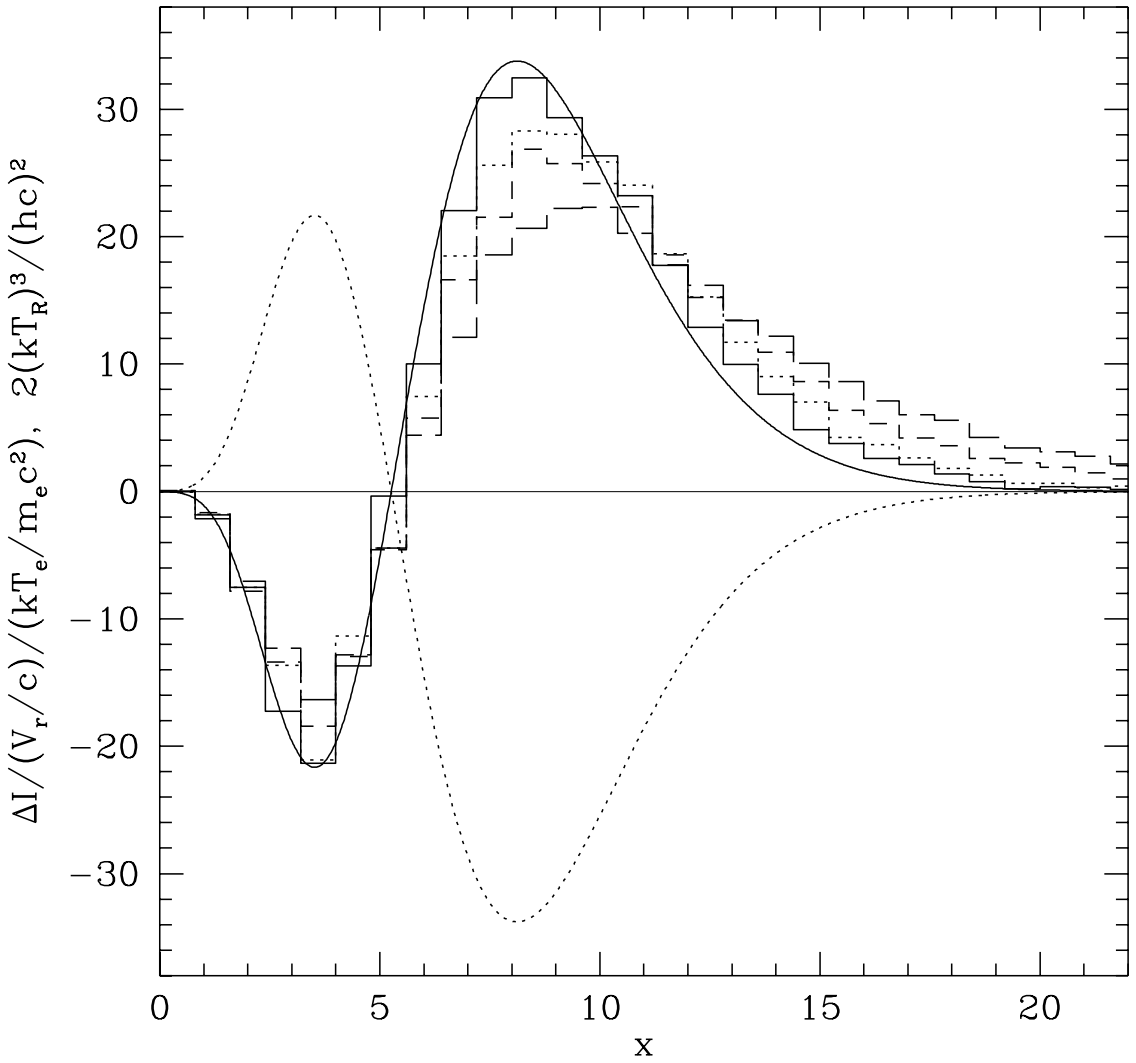


Figure 11: The spectra of the distortion due to the "cross" terms at $V/c = 0.01$, $\mu = 1$, for various values of $kT_e/m_ec^2$: 0.01 (solid histogram), 0.02 (dotted histogram), 0.03 (short-dashed hystogram), 0.05 (long-dashed histogram). The solid line represents the analytical dependence for the correction proportional to $V_r/c \times kT_e/m_ec^2$ calculated from formula (25). For comparison, the same dependence is indicated by the dotted line for $\mu = -1$ (the effect changes its sign, depending on the direction of motion of the cluster).

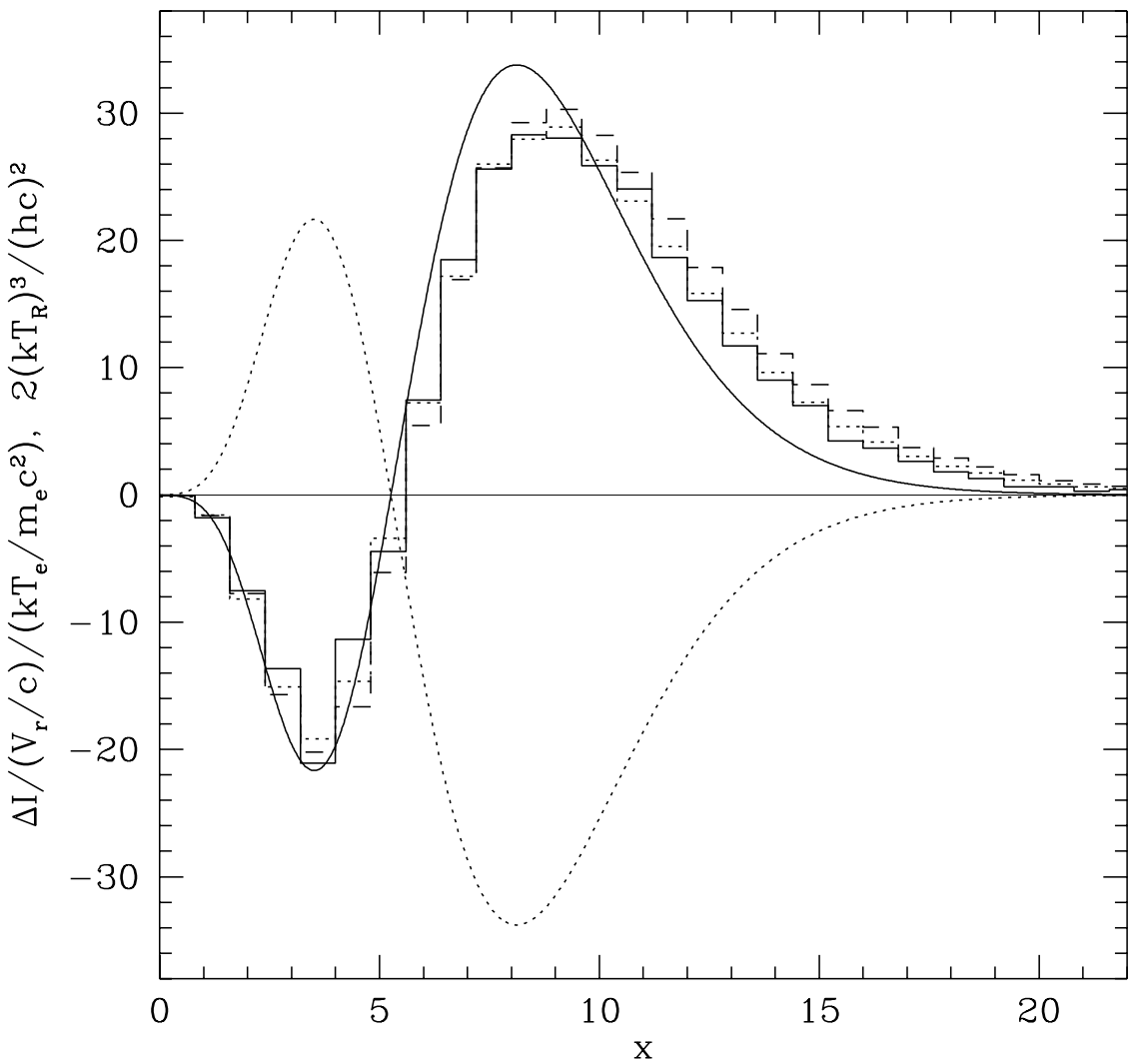


Figure 12: The same as Fig. 11, but for a fixed temperature, $kT_e/m_ec^2 = 0.02$, and various velocities: $V/c = 0.01$ (solid histogram), 0.02 (dotted histogram), 0.05 (dashed histogram).

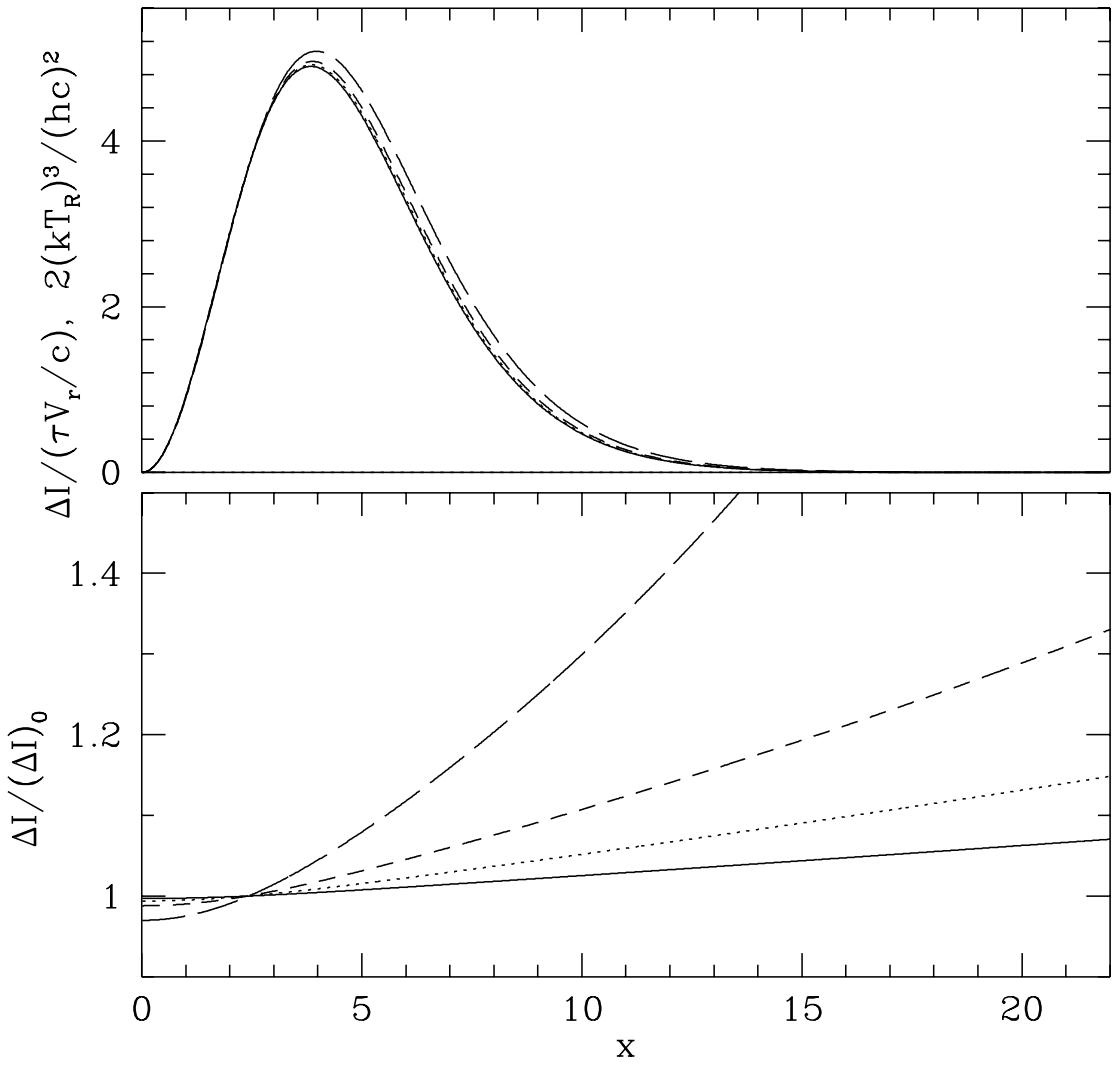


Figure 13: (a) The distortion spectrum in the direction of a moving cluster with cold gas ($kT_e/m_ec^2 \ll V_r/c$) for various peculiar velocities: $V/c = 0.005$ (solid line), 0.01 (dotted line), 0.02 (short dashes), 0.05 (long dashes). The cluster moves toward the observer ($\mu = 1$). (b) The corresponding ratio of the total kinematic effect to that calculated from formula (2).